

References

- 1 Carter CL, Allen C, Henson DE *et al.* Relation of tumour size, lymph node status, and survival in 24,740 breast cancer cases. *Cancer* 1989; **63**: 181–7.
- 2 Elston CW, Ellis IO. Pathological prognostic factors in breast cancer. I. The value of histopathological grade in breast cancer: experience from a large study with long-term follow-up. *Histopathology* 1991; **19**: 403–10.
- 3 Lee AHS, Pinder SE, Macmillan RD *et al.* Prognostic value of lymph vascular invasion in women with lymph node negative invasive breast carcinoma. *Eur J Cancer* 2006; **42**: 357–62.
- 4 Bauer KR, Brown M, Cress RD *et al.* Descriptive analysis of estrogen receptor (ER)-negative, progesterone receptor (PR)-negative, and HER2-negative invasive breast cancer, the so-called triple-negative phenotype: a population-based study from the California cancer Registry. *Cancer* 2007; **109**: 1721–8.
- 5 Tamaki K, Sasano H, Ishida T *et al.* Comparison of core needle biopsy (CNB) and surgical specimens for accurate preoperative evaluation of ER, PgR and HER2 status of breast cancer patients. *Cancer Sci* 2010; **101**: 2074–9.
- 6 Tamaki K, Sasano H, Ishida T *et al.* The correlation between ultrasonographic findings and pathologic features in breast disorders. *Jpn J Clin Oncol* 2010; **40**: 905–12.
- 7 Luck AA, Evans AJ, James JJ *et al.* Breast carcinoma with basal phenotype: mammographic findings. *AJR Am J Roentgenol* 2008; **191**: 346–51.
- 8 Evans AJ, Pinder SE, James JJ *et al.* Is mammographic spiculation an independent, good prognostic factor in screening detected invasive breast cancer? *AJR Am J Roentgenol* 2006; **187**: 1377–80.
- 9 Lee SH, Cho N, Kim SJ *et al.* Correlation between high resolution dynamic MR features and prognostic factors in breast cancer. *Korean J Radiol* 2008; **9**: 10–8.
- 10 Kim SH, Seo BK, Lee J *et al.* Correlation of ultrasound findings with histology, tumor grade, and biological markers in breast cancer. *Acta Oncol* 2008; **47**: 1531–8.
- 11 Amano G, Ohuchi N, Ishibashi T *et al.* Correlation of three-dimensional magnetic resonance imaging with precise histopathological map concerning carcinoma extension in the breast. *Breast Cancer Res Treat* 2000; **60**: 43–55.
- 12 Takase K, Furuta A, Harada N *et al.* Assessing the extent of breast cancer using multidetector row helical computed tomography. *J Comput Assist Tomogr* 2006; **30**: 479–85.
- 13 Harada-Shoji N, Yamada T, Ishida T *et al.* Usefulness of lesion image mapping with multidetector-row helical computed tomography using a dedicated skin marker in breast-conserving surgery. *Eur Radiol* 2009; **19**: 868–74.
- 14 Tavassoli FA, Devilee P. *World Health Organization Classification of Tumors. Tumor of the Breast and Females Genital Organs.* Lyon: IARC Press, 2003.
- 15 Rosen PP. *Rosen's Breast Pathology*, 3rd edn. Philadelphia, PA, USA: Lippincott Williams & Wilkins, 2009.
- 16 Allred DC, Harvey JM, Berardo M, Clark GM. Prognostic and predictive factors in breast cancer by immunohistochemical analysis. *Mod Pathol* 1998; **11**: 155–68.
- 17 Wolff AC, Hammond MH, Schwartz JN *et al.* American Society of Clinical Oncology/College of American Pathologists guideline recommendations for human epidermal growth factor receptor 2 testing in breast cancer. *J Clin Oncol* 2007; **25**: 118–45.
- 18 Goldhirsch A, Ingle JN, Gelber RD *et al.* Thresholds for therapies: highlights of the St Gallen International Expert Consensus on the primary therapy of early breast cancer 2009. *Ann Oncol* 2009; **20**: 1319–29.
- 19 Jalava P, Kuopio T, Juntti-Patinen L *et al.* Ki67 immunohistochemistry: a valuable marker in prognostication but with a risk of misclassification: proliferation subgroups formed based on Ki67 immunoreactivity and standardized mitotic index. *Histopathology* 2006; **48**: 674–82.
- 20 Uematsu T, Kasami M, Yuen S. Triple-negative breast cancer: correlation between MR imaging and pathologic findings. *Radiology* 2009; **250**: 638–47.
- 21 Inoue M, Sano T, Watai R *et al.* Dynamic multidetector CT of breast tumors: diagnostic features and comparison with conventional techniques. *AJR Am J Roentgenol* 2003; **181**: 679–86.
- 22 Jeh SK, Kim SH, Kim HS *et al.* Correlation of the apparent diffusion coefficient value and dynamic magnetic resonance imaging findings with prognostic factors in invasive ductal carcinoma. *J Magn Reson Imaging* 2011; **33**: 102–9.

Nucleobindin 2 in human breast carcinoma as a potent prognostic factor

Shiho Suzuki,¹ Kiyoshi Takagi,^{1,5} Yasuhiro Miki,² Yoshiaki Onodera,² Jun-ichi Akahira,² Akiko Ebata,^{2,3} Takanori Ishida,³ Mika Watanabe,⁴ Hironobu Sasano^{2,4} and Takashi Suzuki¹

Departments of ¹Pathology and Histotechnology, ²Anatomic Pathology, ³Surgical Oncology, Tohoku University Graduate School of Medicine, Sendai; ⁴Department of Pathology, Tohoku University Hospital, Sendai, Japan

(Received June 20, 2011/Revised September 15, 2011/Accepted September 27, 2011/Accepted manuscript online October 11, 2011/Article first published online November 17, 2011)

It is well-known that estrogens immensely contribute to the progression of human breast carcinoma, but their detailed molecular mechanisms remain largely unclear. In this study, we identified nucleobindin 2 (*NUCB2*) as a gene associated with recurrence based on microarray data of estrogen receptor (ER)-positive breast carcinoma cases ($n = 10$), and subsequent *in vitro* study showed that *NUCB2* expression was upregulated by estradiol in ER-positive MCF-7 cells. However, *NUCB2* has not yet been examined in breast carcinoma, and its significance remains unknown. Therefore, we further examined the biological functions of *NUCB2* in breast carcinoma using immunohistochemistry and *in vitro* studies. *NUCB2* immunoreactivity was detected in carcinoma cells in 77 of 161 (48%) breast cancer cases, and positively associated with lymph node metastasis and ER status of the patients. In addition, *NUCB2* status was significantly associated with an increased risk of recurrence and adverse clinical outcome of the patients using both univariate and multivariate analyses. Results of siRNA transfection experiments showed that *NUCB2* significantly increased cell proliferation, and migration and invasion properties in both MCF-7 and ER-negative SK-BR-3 cells. These results suggest that *NUCB2* is up-regulated by estrogens and plays an important role, especially in the process of metastasis, in breast carcinomas. *NUCB2* status is considered a potent prognostic factor in human breast cancer. (*Cancer Sci* 2012; 103: 136–143)

Breast cancer is one of the most common malignancies in women. Estrogens play an important role in the progression of breast cancer through an interaction with ER, and ER is positive in approximately two-thirds of breast carcinoma cases. The great majority of ER-positive breast carcinomas respond to endocrine therapy such as tamoxifen and aromatase inhibitors, but it is also true that some of these carcinomas acquire clinical resistance to endocrine therapy.^(1,2)

Estrogen receptor activates the transcription of various target genes in a ligand-dependent manner by binding EREs located in the promoter region. Various estrogenic functions are characterized by the expression patterns of these genes, which make it extremely important to examine the expression and roles of estrogen-responsive genes to obtain a better understanding of estrogenic actions such as progression, recurrence, and resistance to endocrine therapy.⁽³⁾ Various estrogen-responsive genes have been identified in breast carcinoma,^(4,5) but their detailed clinical significance and/or function remain unclear in a great majority of these genes. Therefore, in this study, we first studied the expression profiles of genes containing ERE in ER-positive breast carcinoma tissues based on microarray data, and identified *NUCB2* as a possible gene associated with recurrence in these patients.

Nucleobindin 2 has a characteristic constitution of functional domains, such as a signal peptide, a Leu/Ile rich region, two Ca²⁺ binding EF-hand domains separated by an acidic amino acid-rich region, and a leucine zipper,^(6,7) and has a wide variety of basic cellular functions.^(8–10) However, to the best of our

knowledge, *NUCB2* has not yet been studied in breast carcinoma. Therefore, we examined *NUCB2* in breast carcinoma using immunohistochemistry and *in vitro* studies to explore its clinical and biological significance.

Materials and Methods

Patients and tissues. Two sets of tissue specimens were evaluated in this study. As a first set, 10 specimens of ER-positive breast carcinoma were obtained from women (age range, 48–74 years) who underwent surgical treatment in 2001 or 2002 in the Department of Surgery, Tohoku University Hospital (Sendai, Japan). All patients received tamoxifen therapy after surgery. The status of recurrence was evaluated whether the first locoregional recurrence or distant metastasis was detected within the follow-up time after surgery (mean, 80 months; range, 37–204 months) or not. These specimens were stored at -80°C for microarray analysis.

As a second set, 161 specimens of invasive ductal carcinoma of human breast were obtained from women who underwent surgical treatment between 1984 and 1997 in the Department of Surgery, Tohoku University Hospital. The patients did not receive chemotherapy, irradiation, or hormonal therapy before the surgery. Review of the charts revealed that 125 patients received adjuvant chemotherapy, 66 patients received tamoxifen therapy, and 12 patients received radiation therapy following surgery. The clinical outcome of the patients was evaluated by disease-free and breast cancer-specific survival. The mean age was 54 years (range, 22–81 years), and the mean follow-up time was 103 months (range, 3–157 months). Mitotic score and histological grade were evaluated according to a previous report.⁽¹¹⁾ All the specimens were fixed in 10% formalin and embedded in paraffin wax.

Research protocols for this study were approved by the Ethics Committee at Tohoku University School of Medicine (Sendai, Japan).

Laser capture microdissection/microarray analysis. Gene expression profiles of breast carcinoma cells in the first set ($n = 10$) were examined using microarray analysis. Gene expression profile data was assembled previously.^(12,13) Briefly, approximately 5000 breast carcinoma cells were laser transferred from the frozen section, and total RNA was subsequently extracted. In this study, we focused on the expression of 519 genes identified to have a functional ERE by Bourdeau *et al.*⁽¹⁴⁾

Immunohistochemistry. Rabbit polyclonal antibody for *NUCB2* and *HER2* (A0485) were purchased from Aviva Systems Biology (San Diego, CA, USA) and Dako (Carpinteria, CA, USA), respectively. Monoclonal antibodies for ER (ER1D5), PR (MAB429), and Ki-67 (MIB1) were purchased

⁵To whom correspondence should be addressed.
E-mail: k-takagi@med.tohoku.ac.jp

from Immunotech (Marseille, France), Chemicon (Temecula, CA, USA), and Dako, respectively.

A Histofine Kit (Nichirei, Tokyo, Japan), which incorporates the streptavidin–biotin amplification method, was used. The antigen–antibody complex was visualized with 3,3'-diaminobenzidine and counterstained with hematoxylin. Human tissue of the stomach was used as a positive control for NUCB2 antibody,⁽¹⁵⁾ and normal rabbit IgG was used instead of the primary antibody, as a negative control of NUCB2 immunostaining.

NUCB2 immunoreactivity was detected in the cytoplasm of breast carcinoma cells, and the cases that had more than 10% of positive carcinoma cells were considered positive for NUCB2 status. Immunoreactivity for ER, PR, and Ki-67 was detected in the nucleus, and the immunoreactivity was evaluated in more than 1000 carcinoma cells for each case. The percentage of immunoreactivity, that is, the LI, was determined. Cases with an ER LI or PR LI of more than 10% were considered ER- or PR-positive breast carcinoma, respectively, according to a previous report.⁽¹⁶⁾

Immunoblotting. The protein of MCF-7 cells was extracted using M-PER Mammalian Protein Extraction Reagent (Pierce Biotechnology, Rockford, IL, USA) with Halt Protease Inhibitor Cocktail (Pierce Biotechnology). Twenty micrograms of the protein (whole cell extracts) was subjected to SDS-PAGE (10% acrylamide gel). Following SDS-PAGE, proteins were transferred onto Hybond-P PVDF membrane (GE Healthcare, Chalfont St Giles, UK). Primary antibody was the same anti-NUCB2 antibody used in the immunohistochemistry (Aviva Systems Biology). Antibody–protein complexes on the blots were detected using ECL Plus Western blotting detection reagents (GE Healthcare), and the protein bands were visualized with a LAS-1000 image analyzer (Fuji Photo Film, Tokyo, Japan).

Real-time PCR. Total RNA was extracted using TRIzol reagent (Invitrogen, Carlsbad, CA, USA), and cDNA was synthesized using a QuantiTect reverse transcription Kit (Qiagen, Hilden, Germany). Real-time PCR was carried out using the LightCycler System and FastStart DNA Master SYBR Green I (Roche Diagnostics, Mannheim, Germany). The primer sequences of NUCB2 and the ribosomal protein L13A (RPL13A) were: NUCB2, 5'-AAAGAAGAGCTACAACGTCA-3' (forward) and 5'-GTGGCTCAAACCTCAATTC-3' (reverse); and RPL13A, 5'-CCTGGAGGAGAAGAGGAAAGAGA-3' (forward) and 5'-TTGAGGACCTGTGTATTGTCAA-3' (reverse). The NUCB2 mRNA level was calculated as the ratio of the RPL13A mRNA level.

Small interfering RNA transfection. Small interfering RNA for NUCB2 was purchased from Ambion (Austin, TX, USA). The target sequences of siRNA against NUCB2 were as follows: si1, 5'-UAUCUUCGCACUUCCACAGGGUGA-3' (sense) and 5'-UCACCCUGUGGAAAGUGCGAAGAU-3' (anti-sense); and si2, 5'-UUGAUUAGCAUAUCUAAAUCUGUGG-3' (sense) and 5'-CCACAGAUUUAGAUUGCUAUAUCA-3' (anti-sense). In addition, medium GC duplex #2 (Invitrogen) was also used as a negative control (siC). The siRNA was transfected using HiperFect transfection reagent (Qiagen).

Cell proliferation, migration, and invasion assays. MCF-7 and SK-BR-3 cells were transfected with NUCB2-specific siRNA or control siRNA in a 96-well culture plate. Three days after transfection, the cell number was evaluated using a Cell Counting Kit-8 (Dojindo, Kumamoto, Japan).

The cell migration assay was carried out using a 24-well plate and Chemotaxicell (8 μ m pore size; Kurabo, Osaka, Japan) according to a previous report.⁽¹⁷⁾ MCF-7 and SK-BR-3 cells were plated at the upper chamber, and the cells on the upper surface of the membrane were removed after incubation for 72 h. The migration ability was evaluated as an average number of cells in five middle power fields ($\times 200$) randomly selected on the lower surface of the membrane.

The cell invasion assay was carried out using a modified migration assay. The upper surface of the membrane of a Chemotaxicell was coated with 80 mg/cm² of Matrigel basement membrane matrix (BD Biosciences, Heidelberg, Germany), and the invasion ability was evaluated as the total number of cells on the lower surface of the membrane.

Results

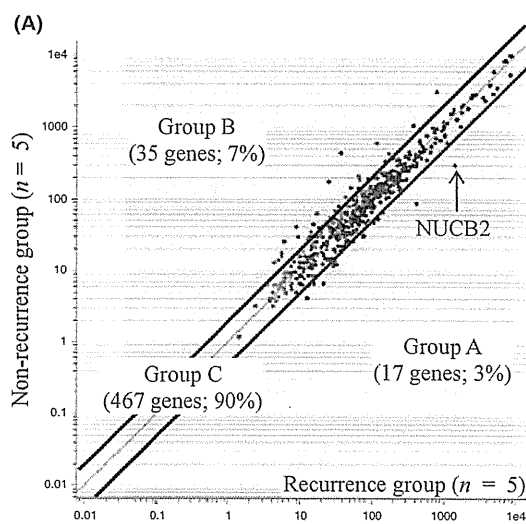
Comparison of gene expression profiles between recurrent and non-recurrent groups of breast carcinoma patients. The microarray data used in this study are available through the National Center for Biotechnology Information Gene Expression Omnibus database (accession GSE11965, <http://www.ncbi.nlm.nih.gov/geo>). In this analysis, when the expression ratio of a gene in the recurrence group compared to that in the non-recurrence group was more than 2.0 or <0.5, we determined that the gene was predominantly expressed in the recurrence or non-recurrence group, respectively.

As shown in Figure 1(A), of the 519 genes examined, the number of genes predominantly expressed in the recurrence group (group A) was 17 (3%); the number of genes predominantly expressed in the non-recurrence group (group B) was 35 (7%). A great majority of the genes (467 genes; 90%) had a similar expression level in each of the two groups (ratio 0.5–2.0) (group C). The lists of genes classified in group A and group B are summarized in the right panel of Figure 1(A), and in Table S1. When we carried out gene ontology enrichment analysis between groups A and B (<http://cbl-gorilla.cs.technion.ac.il/>), no significant enriched gene ontology term was detected. Among the genes in Group A, NUCB2 showed the highest ratio (4.9) and expression level, indicating its possible involvement in the recurrence in ER-positive breast carcinoma patients after surgery.

The NUCB2 gene contains functional ERE in the promoter region⁽¹⁴⁾ but the regulation of NUCB2 expression by estradiol has not been investigated in breast carcinoma cells. As shown in Figure 1(B), NUCB2 mRNA expression was significantly increased by estradiol treatment for 3 days in MCF-7 cells. However, the NUCB2 mRNA expression level was significantly lower ($P < 0.05$, and 0.3-fold) than the basal level, when the cells were treated together with estradiol (10 nM) and a potent ER antagonist ICI 182780 (1 μ M). When MCF-7 cells were treated with estradiol (10 nM) and anti-estrogen tamoxifen (10 μ M), the NUCB2 mRNA level was not significantly changed compared to the basal level ($P = 0.10$, and 1.5-fold). Estradiol (10 nM) time-dependently induced NUCB2 mRNA expression in MCF-7 cells (Fig. 1C).

NUCB2 immunolocalization in human breast carcinoma. As shown in Figure 2(A), immunoblot analysis for NUCB2 revealed a specific band (approximately 43 kDa) in MCF-7 cells, which confirmed the specificity of the anti-NUCB2 antibody used in this study.⁽¹⁸⁾ In the immunohistochemistry, NUCB2 immunoreactivity was detected in the cytoplasm of breast carcinoma cells (Fig. 2B). NUCB2 immunoreactivity was weakly and focally detected in the epithelial cells of morphologically normal glands (Fig. 2C), but it was negative in the stroma. In the positive control, NUCB2 was mainly positive in the epithelium of the fundic glands in the stomach (Fig. 2D), as reported previously,⁽¹⁵⁾ whereas no significant immunoreactivity was detected in the same areas of the negative control section (Fig. 2E).

Associations between NUCB2 immunohistochemical status and various clinicopathological parameters in breast carcinomas are summarized in Table 1. Of 161 cases of breast carcinoma examined in this study, 77 (48%) were NUCB2-positive. NUCB2 status was significantly associated with lymph node metastasis ($P = 0.004$) and ER status ($P = 0.002$) of the patients, whereas no significant association was detected in patients' age, menopausal status, clinical stage, tumor size,



Genes classified as Group A		
Fold†	Common name	Gene symbol
4.9	NM_005013	NUCB2
4.8	AI824012	NRIP1
3.2	NM_001557	CXCR2
3.0	X02189	ADA
2.6	NM_001874	CPM
2.5	NM_001228	CASP8
2.4	AK023540	BUB1
2.3	NM_016083	CNR1
2.3	AF109161	CITED2
2.3	NM_016580	PCDH12
2.2	NM_001256	CDC27
2.2	BC005312	HLA-DRB4
2.2	AF149096	TGFA
2.1	NM_006889	CD86
2.1	X63575	ATP2B2
2.1	X81006	TRIM31
2.1	AW157548	IGFBP5

†: Expression ratio in the recurrence group to that in the non-recurrence group.

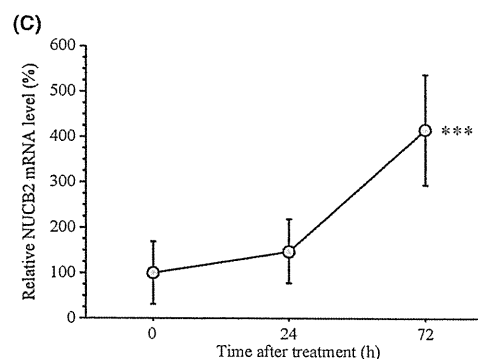
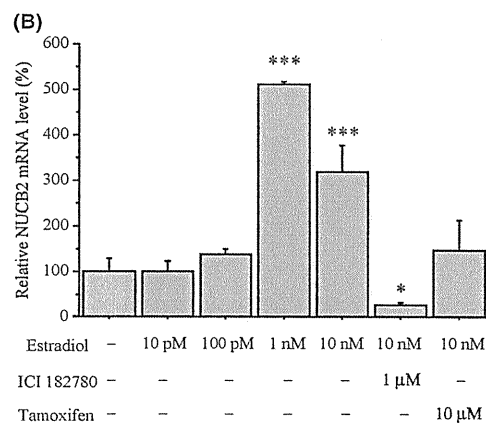


Fig. 1. Nucleobindin 2 (*NUCB2*) as an estrogen-induced gene associated with breast carcinoma. (A) Scatter plot analysis of microarray data for 519 genes containing functional estrogen-responsive element in breast carcinomas comparing the recurrence and non-recurrence group ($n = 5$ in each group). Genes with an expression ratio, recurrence group to non-recurrence group, of more than 2.0 or <0.5 are located outside the diagonal line, and classified as group A or group B, respectively. Genes with a ratio between 2.0 and 0.5 were classified as group C. *NUCB2* showed the highest ratio in these genes (arrow). The right panel summarizes the gene list of group A. (B,C) Effects of estradiol on *NUCB2* mRNA expression. MCF-7 cells were treated with indicated concentrations of estradiol with or without (-) ICI 182780 or tamoxifen for 3 days (B) or treated with estradiol (10 nM) for the indicated period (C). The relative *NUCB2* mRNA level summarized as a ratio (%) compared with the basal level (non-treatment). Data are presented as the mean \pm SD ($n = 3$). * $P < 0.05$ and *** $P < 0.001$ versus non-treatment (left bar) (B) or 0 h (left plot) (C).

histological grade, mitotic score, PR status, *HER2* status, or Ki-67 LI. The positive association between *NUCB2* status and lymph node metastasis was significant regardless of the ER status of these cases ($P = 0.02$) (Table S2). *NUCB2* status was positively associated with Ki-67 LI in the ER-positive group ($P = 0.02$), and was positively correlated with tumor size in ER-negative cases ($P = 0.03$).

When immunohistochemistry was carried out in ductal carcinoma *in situ*, *NUCB2* immunoreactivity was detected in the carcinoma cells (Fig. 2F) in 7 (32%) of 22 cases. The *NUCB2* positivity was 1.5-fold higher in invasive carcinoma (48%) than non-invasive carcinoma (32%), although it did not reach a level of significance ($P = 0.15$).

Association between *NUCB2* status and clinical outcome. In order to thoroughly examine the association between *NUCB2* status and patient prognosis, we excluded stage IV cases and used stage I–III breast carcinoma patients ($n = 141$) in the following analyses. As shown in Figure 3(A), *NUCB2* status

was significantly associated with an increased incidence of recurrence ($P = 0.003$), and the multivariate analysis revealed that lymph node metastasis ($P = 0.01$), ER status ($P = 0.002$), and *NUCB2* status ($P = 0.001$) were independent prognostic factors for disease-free survival with relative risks over 1.0 (Table 2).

A breast cancer-specific survival curve of the patients is summarized in Figure 3(B); a significant correlation ($P = 0.0002$) was detected between *NUCB2* status and adverse clinical outcome in the 141 breast carcinoma patients examined. In the univariate analysis (Table 2), lymph node metastasis ($P = 0.0004$), *NUCB2* status ($P = 0.002$), ER status ($P = 0.003$), histological grade ($P = 0.01$), *HER2* status ($P = 0.01$), and tumor size ($P = 0.02$) were all indicated as significant prognostic variables for breast cancer-specific survival. A following multivariate analysis showed that only *NUCB2* status ($P = 0.0004$) and ER status ($P = 0.01$) were independent prognostic factors with a relative risk over 1.0, whereas lymph node metastasis

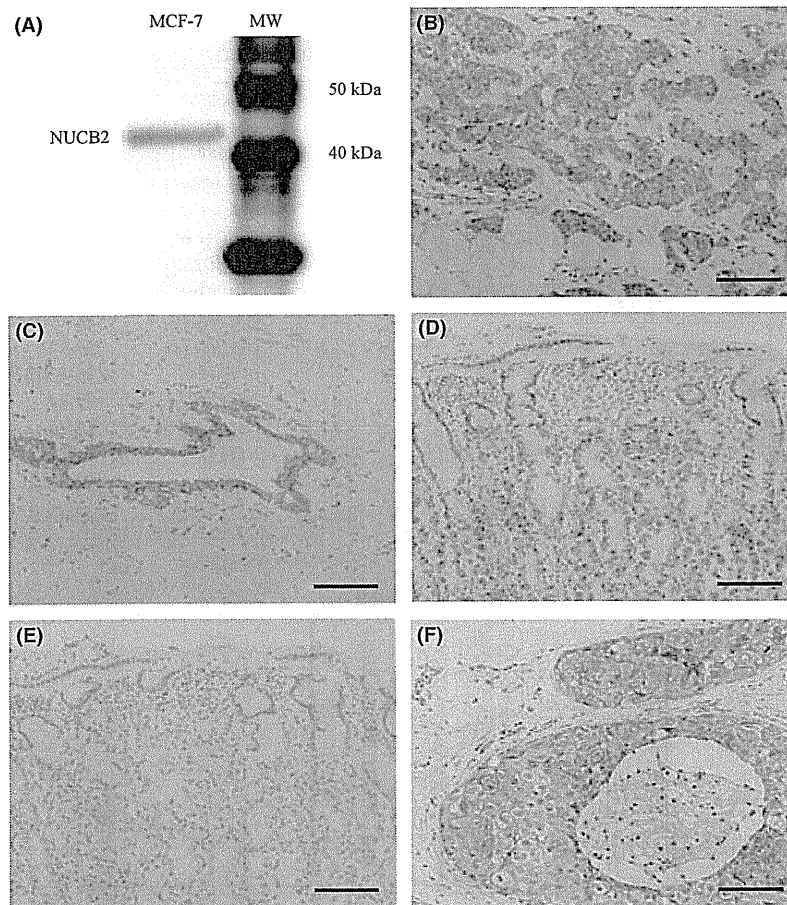


Fig. 2. Immunohistochemistry for nucleobindin 2 (*NUCB2*) in breast carcinoma. (A) Immunoblotting for *NUCB2* in MCF-7 cells. MW, molecular weight. (B) *NUCB2* immunoreactivity was detected in the carcinoma cells of invasive ductal carcinoma. (C) *NUCB2* immunoreactivity was weakly and focally detected in morphologically normal mammary glands. (D) Positive control section of *NUCB2* immunohistochemistry (gastric mucosa). (E) Negative control section of *NUCB2* immunohistochemistry (same area as Fig. 2D). (F) *NUCB2* immunoreactivity was detected in the carcinoma cells of ductal carcinoma *in situ*. Bar = 100 μm .

($P = 0.22$), histological grade ($P = 0.28$), *HER2* status ($P = 0.60$), and tumor size ($P = 0.07$) were not significant.

A similar association between *NUCB2* and worse prognosis was detected regardless of the Ki-67 status ($P = 0.03$ in cases with Ki-67 LI $\geq 10\%$ and $P = 0.04$ in cases with Ki-67 $< 10\%$ for disease-free survival [Fig. 3C]; $P = 0.004$ in cases with Ki-67 LI $\geq 10\%$ and P -value not available cases with Ki-67 $< 10\%$ because no patient died in the *NUCB2*-negative group for breast cancer-specific survival). When the 66 *NUCB2*-positive cases were further categorized into two groups according to immunointensity (++, strongly positive [$n = 16$]; +, modestly positive [$n = 50$]), no significant difference was detected between these two groups ($P = 0.60$ for disease-free survival [Fig. 3D], and $P = 0.49$ for breast cancer-specific survival).

Forty patients with stage I–III disease received tamoxifen therapy following surgery as an adjuvant treatment, and these cases were all positive for ER. *NUCB2* status was also markedly associated with an increased risk of recurrence (Fig. 3E) and worse prognosis (data not shown) in the patients who received tamoxifen therapy, although P -values were not available because no patient had recurrent disease or died in the group of *NUCB2*-negative cases. Significant association between *NUCB2* status and patients' clinical outcome was also detected in the 113 patients who received adjuvant chemotherapy ($P = 0.03$ for disease-free and $P = 0.002$ for breast cancer-specific survival),

38 ER-negative cases ($P = 0.0001$ for disease-free and $P < 0.0001$ for breast cancer-specific survival), or 24 cases with ER LI $< 1\%$ ($P = 0.001$ for disease-free [Fig. 3F] and $P = 0.0004$ for breast cancer-specific survival).

Effects of *NUCB2* expression on cell proliferation and invasion in breast carcinoma cells. The results of our study suggest that *NUCB2* is associated with worse prognosis of breast carcinoma patients regardless of their ER status, although *NUCB2* expression is upregulated by estrogen. In order to further examine the biological functions of *NUCB2* in human breast carcinoma, we transfected specific siRNA for *NUCB2* both in ER-positive MCF-7 and ER-negative SK-BR-3 breast carcinoma cells. The *NUCB2* mRNA expression level was markedly decreased in these cells transfected with specific *NUCB2* siRNA (si1 or si2) at 3 days after transfection compared to cells transfected with control siRNA (siC). The ratio of *NUCB2* mRNA level compared to that in the control siRNA was: MCF-7, 5% (si1) and 8% (si2); and SK-BR-3, 11% (si1) and 12% (si2).

As shown in Figure 4(A), the number of cells was significantly lower in MCF-7 cells transfected with *NUCB2* siRNA ($P < 0.001$ and 0.52-fold in si1, and $P < 0.001$ and 0.64-fold in si2) than in control cells transfected with siC 3 days after the transfection. A similar association was also detected in SK-BR-3 cells under the same conditions ($P < 0.001$ and 0.75-fold in si1, and $P < 0.001$ and 0.81-fold in si2). Figure 4(B) shows the

Table 1. Association between nucleobindin 2 (*NUCB2*) immunohistochemical status and clinicopathological parameters in 161 breast carcinomas

	<i>NUCB2</i> status		<i>P</i> -value
	Positive (<i>n</i> = 77)	Negative (<i>n</i> = 84)	
Age† (years)	53.9 ± 1.4	54.4 ± 1.2	0.770
Menopausal status (%)			
Premenopausal	31 (19)	35 (22)	0.860
Postmenopausal	46 (29)	49 (30)	
Stage (%)			
I	18 (11)	24 (15)	0.730
II	38 (24)	43 (27)	
III	10 (6)	8 (5)	
IV	11 (7)	9 (6)	
Tumor size† (cm)	3.4 ± 0.4	3.4 ± 0.4	0.990
Lymph node metastasis (%)			
Positive	41 (25)	26 (16)	0.004
Negative	36 (22)	58 (36)	
Histological grade (%)			
1 (well)	20 (12)	24 (15)	0.930
2 (moderate)	30 (19)	31 (19)	
3 (poor)	27 (17)	29 (18)	
Mitotic score (%)			
1 (low)	33 (20)	43 (27)	0.570
2 (moderate)	22 (14)	21 (13)	
3 (high)	22 (14)	20 (12)	
ER status (%)			
Positive	65 (40)	53 (33)	0.002
Negative	12 (7)	31 (19)	
PR status (%)			
Positive	55 (34)	51 (32)	0.150
Negative	22 (14)	33 (20)	
HER2 status (%)			
Positive	22 (14)	24 (15)	0.990
Negative	55 (34)	60 (37)	
Ki-67 LI† (%)	23.6 ± 1.8	21.1 ± 2.1	0.380

†Data are presented as the mean ± SEM. All other values represent the number of cases and percentage. ER, estrogen receptor; LI, labeling index; PR, progesterone receptor. *P*-values <0.05 were considered significant, indicated in bold.

results of the migration assay. The number of migrated cells was significantly lower in both MCF-7 cells ($P < 0.001$ and 0.11-fold in si1, and $P < 0.001$ and 0.43-fold in si2) and SK-BR-3 cells ($P < 0.001$ and 0.36-fold in si1, and $P < 0.001$ and 0.31-fold in si2) transfected with *NUCB2* siRNA than in those transfected with control siRNA at 1 day (MCF-7) or 2 days (SK-BR-3) after the transfection. Moreover, the number of invaded cells was also significantly lower in the cells transfected with *NUCB2* siRNA (MCF-7, $P < 0.05$ and 0.21-fold in si1 and $P < 0.05$ and 0.29-fold in si2; SK-BR-3, $P < 0.01$ and 0.66-fold in si1 and $P < 0.001$ and 0.47-fold in si2) (Fig. 4C,D).

Discussion

Gene expression profiling is an important method to predict the likelihood of recurrence of disease in breast cancer patients,⁽¹⁹⁾ in addition to conventional clinical and histopathological examination. A multigene classifier associated with recurrence has been proposed for breast carcinoma patients by several research groups,^(19–21) and molecular-based diagnostic systems have been developed, such as MammaPrint⁽²²⁾ and Oncotype DX,⁽²³⁾ as well as the genomic grade index.⁽²⁴⁾ However, the selected genes vary markedly between these diagnostic systems, which may be partly due to the fact that they use different platforms for the analysis of gene expression. In addition, the biological

functions have remained largely unknown in a great majority of these genes. In our present study, the results of microarray analysis revealed 17 genes that are potentially associated with recurrence in ER-positive breast carcinoma patients (group A in Fig. 1A). Among these, *IGFBP5* (insulin-like growth factor-binding protein 5) was reported to play an important role in breast carcinoma metastasis,^(25,26) and is included in MammaPrint. In addition, *TGFA* (transforming growth factor α), a member of the epidermal growth factor family, is well-known to be involved in cellular proliferation and carcinogenesis.⁽²⁷⁾ The kinetochore-bound protein kinase *BUB1* (budding uninhibited by benzimidazoles 1) is a possible link to tumorigenesis.⁽²⁸⁾ *NUCB2* showed the highest expression ratio in this study, but this gene has not been listed in any multigene classifiers predicting breast carcinoma recurrence, nor has it been examined in breast carcinoma, to the best of our knowledge.

In this study, we first showed that *NUCB2* immunoreactivity was detected in 48% of breast carcinoma cases, although levels were almost negligible in morphologically normal mammary glands. *NUCB2* is known to mainly express in key hypothalamic nuclei with proven roles in energy homeostasis.⁽⁹⁾ Moreover, recent investigations have indicated that *NUCB2* is also expressed in various human peripheral tissues, including the stomach, pancreas, reproductive organs, and adipose tissues, with relevant metabolic functions, suggesting that *NUCB2* signaling might participate in adaptive responses and in the control of body functions gated by the state of energy reserves.⁽²⁹⁾ However, *NUCB2* expression in carcinoma has only been examined in the stomach; Kalnina *et al.*⁽¹⁵⁾ reported that *NUCB2* immunoreactivity was not detected in carcinoma cells in 15 gastric carcinoma cases examined. The relatively wide distribution of *NUCB2* immunoreactivity in our present study suggests that *NUCB2* plays an important role in human breast carcinoma.

Bourdeau *et al.*⁽¹⁴⁾ evaluated genome-wide identification of EREs in humans, and identified a functional ERE element at 8257 bp from the most upstream mRNA 5'-end of the *NUCB2* gene. In our present study, *NUCB2* immunohistochemical status was positively associated with ER status in breast carcinoma tissue, and *NUCB2* mRNA was significantly upregulated by estradiol in MCF-7 cells through ER. Therefore, *NUCB2* is considered one of the estrogen-induced genes in breast carcinoma cells. Results of our present study also indicated the presence of *NUCB2* in 12 of 43 (28%) ER-negative breast carcinoma cases; it might be the case that *NUCB2* was induced by a low or undetectable level of ER in these cases. However, it is also true that estrogen-mediated induction of *NUCB2* mRNA was relatively slow in MCF-7 cells in our time-course study (Fig. 1C), suggesting that *NUCB2* expression is, at least in a part, induced by secondary responses, although the half-life of mRNA is an important factor in determining how long it takes to detect a change in the mRNA level of a specific gene.⁽⁴⁾ In addition, *NUCB2* is expressed in various human tissues not necessarily considered targets for estrogens, as described above.⁽²⁹⁾ Therefore, other factors than estrogens might be involved in the expression of *NUCB2* in breast carcinoma cells. No information is currently available regarding the regulation mechanisms of *NUCB2* expression to the best of our knowledge, and further research is required.

Previous studies have shown that ICI 182780 possesses a greater ability to suppress estrogen-sensitive gene expression and greater antitumor activity than tamoxifen in breast carcinoma.⁽³⁰⁾ This is partly due to the fact that ICI 182780 does not have agonistic ER activity and reduces steady-state levels of ER by increasing the turnover of the protein, whereas tamoxifen does possess partial agonistic ER activity.⁽³¹⁾ In our study, ICI 182780 was superior to tamoxifen in suppressing estradiol-mediated induction of *NUCB2* mRNA in MCF-7 cells (Fig. 1B), which is consistent with previous studies.

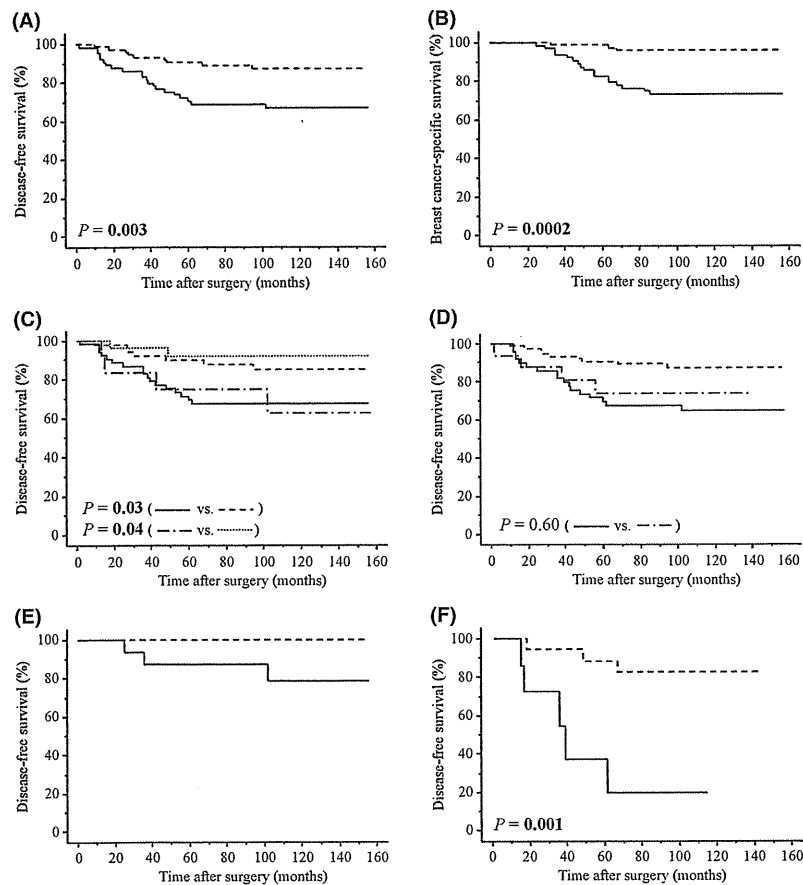


Fig. 3. Disease-free and breast cancer-specific survival of 141 breast carcinoma patients according to nucleobindin 2 (*NUCB2*) status. (A,B) *NUCB2* status was significantly associated with an increased risk of recurrence ($P = 0.003$) (A) and worse prognosis ($P = 0.0002$) (B). Solid line, positive for *NUCB2* ($n = 66$); dashed line, negative for *NUCB2* ($n = 75$). (C) Disease-free survival curve according to *NUCB2*/Ki-67 status. Solid line, positive for *NUCB2*/Ki-67 labeling index (LI) $\geq 10\%$ ($n = 54$); dashed line, positive for *NUCB2*/Ki-67 LI $< 10\%$ ($n = 12$); dotted line, negative for *NUCB2*/Ki-67 LI $\geq 10\%$ ($n = 50$); dot-dashed line, negative for *NUCB2*/Ki-67 LI $< 10\%$ ($n = 25$). (D) Disease-free survival curve according to *NUCB2* immunointensity. Solid line, strongly positive ($n = 16$); dashed line, modestly positive ($n = 50$); dot-dashed line, negative ($n = 75$). (E) *NUCB2* status was associated with recurrence in 40 patients who received tamoxifen therapy. P -value not available as there were no patients with recurrent disease in the *NUCB2*-negative group. Solid line, positive for *NUCB2* ($n = 16$); dashed line, negative for *NUCB2* ($n = 24$). (F) *NUCB2* status was significantly ($P = 0.001$) associated with recurrence in a group with estrogen receptor labeling index $< 1\%$ ($n = 24$). Solid line, positive for *NUCB2* ($n = 7$); dashed line, negative for *NUCB2* ($n = 17$).

In our present study, *NUCB2* immunoreactivity was positively associated with the presence of lymph node metastasis in breast carcinoma tissue both in ER-positive and ER-negative cases. In addition, subsequent *in vitro* studies indicated that both MCF-7 and SK-BR-3 cells transfected with siRNA *NUCB2* significantly decreased cell proliferation, and migration and invasion properties. Metastasis is considered as the major cause of treatment failure and death of carcinoma patients. It is a multistep process that involves migration and invasion of carcinoma cells, lymphogenous and/or hematogenous spread, and cell proliferation in the metastatic sites. Previous studies have shown that *NUCB2* has a wide variety of basic cellular functions, including an involvement in the energy homeostasis,⁽⁹⁾ Ca²⁺ homeostasis,⁽⁸⁾ and extracellular tumor necrosis factor receptor type 1 release,⁽¹⁰⁾ although the biological functions have not yet been fully clarified. Results of our present study suggest that *NUCB2* plays a pivotal role, especially in the metastasis of breast carcinomas, and serve as a starting point for clarification of the biological roles of *NUCB2* in breast carcinoma. However, we could not necessarily detect a significant association between *NUCB2* status and mitotic score, Ki-67 LI, or invasion status in the clinical

samples. Therefore, other factors might also play important roles in the processes of proliferation and invasion in breast carcinoma tissues.

In our present study, *NUCB2* status was also significantly associated with recurrence and worse prognosis in breast carcinoma patients, and a similar tendency was also detected in ER-positive patients who received tamoxifen therapy, or in ER-negative cases. In addition, results of multivariate analyses showed that *NUCB2* status was indeed an independent prognostic factor for both recurrence and breast cancer-specific survival. Results of our *in vitro* study indicated that tamoxifen inhibited estradiol-mediated induction of *NUCB2* expression in MCF-7 cells, but the basal expression level of *NUCB2* mRNA still remained. Considering that the *NUCB2* expression level was the highest among the genes predominantly expressed in the recurrence group despite tamoxifen therapy (group A in Fig. 1A), *NUCB2* status in breast carcinoma tissues at the time of surgery might reflect the basal level of *NUCB2* as well as the level induced by estrogens in breast carcinoma cases. Therefore, residual carcinoma cells following surgical treatment in *NUCB2*-positive breast carcinomas could still have the potential to rapidly grow and/or metastasize,

Table 2. Univariate and multivariate analyses of disease-free survival and breast cancer-specific survival in patients with stage I–III breast cancer (n = 141)

Variable	Univariate	Multivariate	
	P-value	P-value	Relative risk (95% CI)
Disease-free survival			
Lymph node metastasis (positive/negative)	<0.0001	0.0100	3.1 (1.3–7.6)
ER status (negative/positive)	0.0020	0.0020	4.8 (1.8–13.0)
<i>NUCB2</i> status (positive/negative)	0.0100	0.0010	4.6 (1.8–11.4)
<i>HER2</i> status (positive/negative)	0.0100	0.6600	ND
Tumor size (≥2.0 cm/<2.0 cm)	0.0200	0.1300	ND
Histological grade (3/1, 2)	0.0900	ND	ND
Ki-67 LI (≥10%/<10%)	0.3500	ND	ND
Menopausal status (pre/post)	0.6400	ND	ND
Breast cancer-specific survival			
Lymph node metastasis (positive/negative)	0.0004	0.2200	ND
<i>NUCB2</i> status (positive/negative)	0.0020	0.0004	12.0 (3.0–47.7)
ER status (negative/positive)	0.0030	0.0100	5.6 (1.5–20.7)
Histological grade (3/1,2)	0.0100	0.2800	ND
<i>HER2</i> status (positive/negative)	0.0100	0.6000	ND
Tumor size (≥2.0 cm/<2.0 cm)	0.0200	0.0700	ND
Ki-67 LI (≥10%/<10%)	0.1000	ND	ND
Menopausal status (post/pre)	0.7800	ND	ND

Data considered significant ($P < 0.05$) in the univariate analyses are shown in bold, and were examined in the multivariate analyses. CI, confidence interval; ER, estrogen receptor; LI, labeling index; ND, not done; *NUCB2*, nucleobindin 2; PR, progesterone receptor.

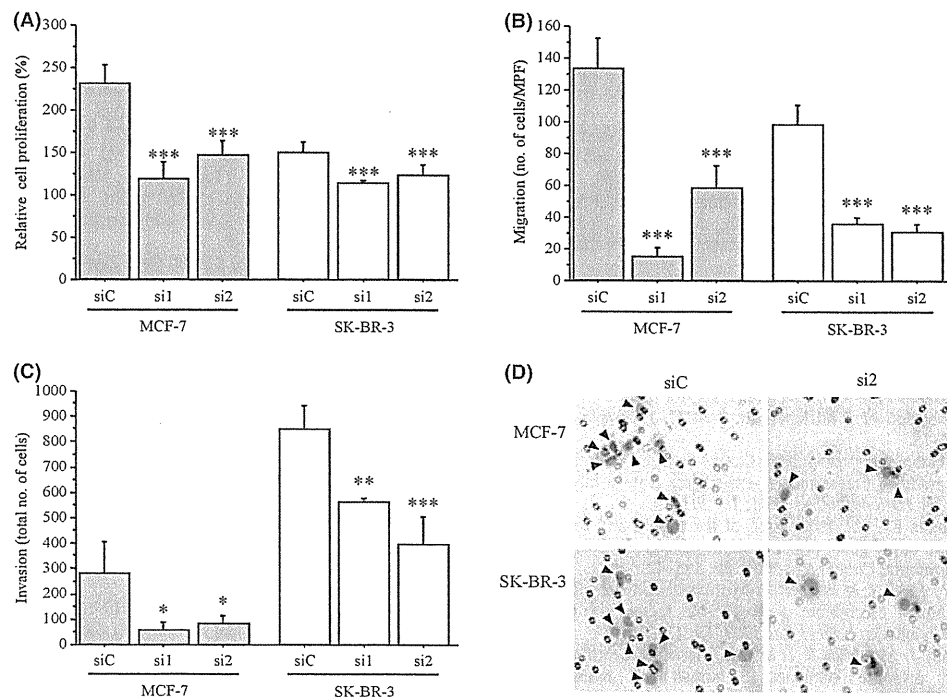


Fig. 4. Effects of nucleobindin 2 (*NUCB2*) on proliferation (A), and migration (B) and invasion (C,D) properties in breast carcinoma cells. (A–C) MCF-7 (gray bar) and SK-BR-3 (open bar) were transfected with *NUCB2*-specific siRNA (si1, si2) or control siRNA (siC). The relative cell proliferation was evaluated as a ratio (%) compared to that at 0 day after treatment (A). Migration ability was evaluated as an average number of cells in five middle power fields (MPF) ($\times 200$) on the lower surface of the membrane (B). Invasion ability was evaluated as the total number of cells (C). Data are presented as the mean \pm SD ($n = 6$ [A]; $n = 3$ [B,C]). * $P < 0.05$; ** $P < 0.01$; *** $P < 0.001$ versus control cells (left bar). (D) Representative microphotographs of results of invasion assay. Invaded carcinoma cells (arrows) were observed with 8 μ m-sized pore. Nuclei stained with hematoxylin. When MCF-7 (upper panel) and SK-BR-3 (lower panel) cells were transfected with *NUCB2*-specific siRNA (si2) (right panel), the number of invading cells was decreased compared to the corresponding control (transfection with control siRNA [siC], left panel). Bar = 100 μ m.

despite the fact that tamoxifen therapy partially suppresses the *NUCB2* expression level, thereby resulting in an increased recurrence and poor prognosis in these patients.

In summary, *NUCB2* was newly identified as a gene associated with recurrence in breast carcinoma patients by microarray analysis, and a subsequent *in vitro* study indicated that *NUCB2*

expression was upregulated by estrogen in MCF-7 cells. *NUCB2* immunoreactivity was detected in 48% of breast carcinoma tissues, and was an independent prognostic factor of the patients. Results of further *in vitro* studies showed that *NUCB2* significantly increased the proliferation activity, and migration and invasion properties both in MCF-7 and SK-BR-3 cells. These findings suggest that *NUCB2* plays an important role, especially in the metastasis of breast carcinoma, and *NUCB2* status in primary breast carcinoma is reasonably considered a potent prognostic factor.

Acknowledgments

We appreciate the skillful technical assistance of Mr. Katsuhiko Ono (Department of Anatomic Pathology, Tohoku University Graduate

School of Medicine, Sendai, Japan). This work was partly supported by a Grant-in-Aid for Scientific Research from the Japanese Ministry of Education, Culture, Sports, Science and Technology.

Disclosure Statement

The authors have no conflicts of interest.

Abbreviations

ER	estrogen receptor
ERE	estrogen-responsive element
LI	labeling index
NUCB2	nucleobindin 2
PR	progesterone receptor

References

- Jordan VC. Fourteenth Gaddum Memorial Lecture. A current view of tamoxifen for the treatment and prevention of breast cancer. *Br J Pharmacol* 1993; **110**: 507–17.
- Ali S, Coombes RC. Endocrine-responsive breast cancer and strategies for combating resistance. *Nat Rev Cancer* 2002; **2**: 101–12.
- Suzuki T, Inoue A, Miki Y *et al*. Early growth responsive gene 3 in human breast carcinoma: a regulator of estrogen-mediated invasion and a potent prognostic factor. *Endocr Relat Cancer* 2007; **14**: 279–92.
- Frasor J, Danes JM, Komm B, Chang KC, Lyttle CR, Katzenellenbogen BS. Profiling of estrogen up- and down-regulated gene expression in human breast cancer cells: insights into gene networks and pathways underlying estrogenic control of proliferation and cell phenotype. *Endocrinology* 2003; **144**: 4562–74.
- Hayashi SI, Eguchi H, Tanimoto K *et al*. The expression and function of estrogen receptor alpha and beta in human breast cancer and its clinical application. *Endocr Relat Cancer* 2003; **10**: 193–202.
- Miura K, Titani K, Kurosawa Y, Kanai Y. Molecular cloning of nucleobindin, a novel DNA-binding protein that contains both a signal peptide and a leucine zipper structure. *Biochem Biophys Res Commun* 1992; **187**: 375–80.
- Barnikol-Watanabe S, Gross NA, Götz H *et al*. Human protein NEFA, a novel DNA binding/EF-hand/leucine zipper protein. Molecular cloning and sequence analysis of the cDNA, isolation and characterization of the protein. *Biol Chem Hoppe Seyler* 1994; **375**: 497–512.
- Taniguchi N, Taniura H, Niinobe M *et al*. The postmitotic growth suppressor necdin interacts with a calcium-binding protein (NEFA) in neuronal cytoplasm. *J Biol Chem* 2000; **275**: 31674–81.
- Oh IS, Shimizu H, Satoh T *et al*. Identification of nesfatin-1 as a satiety molecule in the hypothalamus. *Nature* 2006; **443**: 709–12.
- Islam A, Adamik B, Hawari FI *et al*. Extracellular TNFR1 release requires the calcium-dependent formation of a nucleobindin 2-ARTS-1 complex. *J Biol Chem* 2006; **281**: 6860–73.
- Elston CW, Ellis IO. Pathological prognostic factors in breast-cancer. 1. The value of histological grade in breast-cancer - experience from a large study with long-term follow-up. *Histopathology* 1991; **19**: 403–10.
- Miki Y, Suzuki T, Kitada K *et al*. Expression of the steroid and xenobiotic receptor and its possible target gene, organic anion transporting polypeptide-A, in human breast carcinoma. *Cancer Res* 2006; **66**: 535–42.
- Nagasaki S, Suzuki T, Miki Y *et al*. 17 β -hydroxysteroid dehydrogenase type 12 in human breast carcinoma: a prognostic factor via potential regulation of fatty acid synthesis. *Cancer Res* 2009; **69**: 1392–9.
- Bourdeau V, Deschênes J, Me'tivier R *et al*. Genomewide identification of high-affinity estrogen response elements in human and mouse. *Mol Endocrinol* 2004; **18**: 1411–27.
- Kalnina Z, Silina K, Bruvere R *et al*. Molecular characterisation and expression analysis of SEREX-defined antigen NUCB2 in gastric epithelium, gastritis and gastric cancer. *Eur J Histochem* 2009; **53**: 7–18.
- Takagi K, Miki Y, Nagasaki S *et al*. Increased intratumoral androgens in human breast carcinoma following aromatase inhibitor exemestane treatment. *Endocr Relat Cancer* 2010; **17**: 415–30.
- Oka K, Suzuki T, Onodera Y *et al*. Nudix-type motif 2 in human breast carcinoma: a potent prognostic factor associated with cell proliferation. *Int J Cancer* 2011; **128**: 1770–82.
- Ramanjaneya M, Chen J, Brown JE *et al*. Identification of nesfatin-1 in human and murine adipose tissue: a novel depot-specific adipokine with increased levels in obesity. *Endocrinology* 2010; **151**: 3169–80.
- Oh DS, Troester MA, Usary J *et al*. Estrogen-regulated genes predict survival in hormone receptor-positive breast cancers. *J Clin Oncol* 2006; **24**: 1656–64.
- Huang E, Cheng SH, Dressman H *et al*. Gene expression predictors of breast cancer outcomes. *Lancet* 2003; **361**: 1590–6.
- Naoi Y, Kishi K, Tanei T *et al*. Development of 95-gene classifier as a powerful predictor of recurrences in node-negative and ER-positive breast cancer patients. *Breast Cancer Res Treat* 2011; **128**: 633–41.
- van't Veer LJ, Dai H, van de Vijver MJ *et al*. Gene expression profiling predicts clinical outcome of breast cancer. *Nature* 2002; **415**: 530–6.
- Paik S. Development and clinical utility of a 21-gene recurrence score prognostic assay in patients with early breast cancer treated with tamoxifen. *Oncologist* 2007; **12**: 631–5.
- Sotiriou C, Wirapati P, Loi S *et al*. Gene expression profiling in breast cancer: understanding the molecular basis of histologic grade to improve prognosis. *J Natl Cancer Inst* 2006; **98**: 262–72.
- Hao X, Sun B, Hu L *et al*. Differential gene and protein expression in primary breast malignancies and their lymph node metastases as revealed by combined cDNA microarray and tissue microarray analysis. *Cancer* 2004; **100**: 1110–22.
- Li X, Cao X, Li X, Zhang W, Feng Y. Expression level of insulin-like growth factor binding protein 5 mRNA is a prognostic factor for breast cancer. *Cancer Sci* 2007; **98**: 1592–6.
- Booth BW, Smith GH. Roles of transforming growth factor- α in mammary development and disease. *Growth Factors* 2007; **25**: 227–35.
- Klebig C, Korin D, Meraldi P. Bub1 regulates chromosome segregation in a kinetochore-independent manner. *J Cell Biol* 2009; **185**: 841–58.
- García-Galiano D, Navarro VM, Gaytan F, Tena-Sempere M. Expanding roles of NUCB2/nesfatin-1 in neuroendocrine regulation. *J Mol Endocrinol* 2010; **45**: 281–90.
- Osborne CK, Coronado-Heinsohn EB, Hilsenbeck SG *et al*. Comparison of the effects of a pure steroidal antiestrogen with those of tamoxifen in a model of human breast cancer. *J Natl Cancer Inst* 1995; **87**: 746–50.
- Dauvois S, White R, Parker MG. The antiestrogen ICI 182780 disrupts estrogen receptor nucleocytoplasmic shuttling. *J Cell Sci* 1993; **106**: 1377–88.

Supporting Information

Additional Supporting Information may be found in the online version of this article:

Table S1. Genes predominantly expressed in the non-recurrence group, classified as group B.

Table S2. Association between nucleobindin 2 (*NUCB2*) status and clinicopathological parameters according to estrogen receptor status in 161 breast carcinomas.

Please note: Wiley-Blackwell are not responsible for the content or functionality of any supporting materials supplied by the authors. Any queries (other than missing material) should be directed to the corresponding author for the article.

MicroRNA-34b functions as a potential tumor suppressor in endometrial serous adenocarcinoma

Eri Hiroki¹, Fumihiko Suzuki¹, Jun-ichi Akahira², Satoru Nagase¹, Kiyoshi Ito¹, Jun-ichi Sugawara¹, Yasuhiro Miki³, Takashi Suzuki³, Hironobu Sasano³ and Nobuo Yaegashi¹

¹Department of Obstetrics and Gynecology, Tohoku University Graduate School of Medicine, Sendai, Japan

²Department of Pathology, Tohoku Kosei Nenkin Hospital, Sendai, Japan

³Department of Pathology, Tohoku University Graduate School of Medicine, Sendai, Japan

Endometrial serous adenocarcinoma (ESC) is aggressive and carries a poor prognosis. p53 is frequently mutated in ESC. microRNAs (miRNAs) are a direct p53 target and have been implicated in cancer cell behavior. In this study, we compared miRNA expression levels in ESC with the levels in endometrial endometrioid adenocarcinoma (EEC) and normal endometria. Six miRNAs were identified as having aberrant down-regulation specific to ESC with miR-34b being most pronounced. miR-34b was found to have promoter hypermethylation, which when reversed, restored miR-34b expression in the cell lines treated with 5-aza-2'-deoxycytidine (DAC). Ectopic expression of miR-34b in turn inhibited cell growth, migration and most notably invasion. Our findings suggest a relationship among p53 mutation, miR-34b promoter methylation and tumor cell behavior. These effects are likely mediated by the downstream target of miR-34b, the proto-oncogene mesenchymal-epithelial transition factor (MET), a known prognostic factor in endometrial carcinomas. The expression of MET was reduced following the restoration of miR-34b in cell lines. In summary, our data suggest that miR-34b plays a role in the molecular pathogenesis of endometrial cancer.

Introduction

Endometrial serous adenocarcinoma (ESC) accounts for 10% of all endometrial carcinomas. In contrast to the more common Type I endometrial carcinomas, this tumor often presents at an advanced stage with deep myometrial invasion and a high incidence of lymph node involvement. The average age of onset is older than for Type I endometrial carcinoma.¹ The recurrence rate for ESC is high and the 5-year survival rate ranges from 15 to 51%.² The prognosis of ESC is, at best, equivalent to that of Grade III endometrial endometrioid adenocarcinoma (EEC) confined to the uterus.³ The most prominent genetic alteration in ESC, demonstrated in 90% of tumors, is p53 mutation,⁴ which frequently manifests as an accumulation of defective p53 protein.^{5,6} Although p53 mutation is a common genetic alteration in a variety of tumor types, its role in tumorigenesis, particularly in gynecologic cancers, has not been completely elucidated.

Key words: microRNA, miR-34b, MET, endometrial cancer, serous
Additional Supporting Information may be found in the online version of this article.

DOI: 10.1002/ijc.27345

History: Received 23 Dec 2010; Accepted 28 Sep 2011; Online 2 Nov 2011

Correspondence to: Fumihiko Suzuki, Department of Obstetrics and Gynecology, Tohoku University Graduate School of Medicine, 1-1 Seiryō-Machi, Aoba-ku, Sendai 980-8574, Japan, Tel.: +81-22-717-7254, Fax: +81-22-717-7258, E-mail: suzuki62@med.tohoku.ac.jp

Furthermore, conflict exists regarding the utilization of p53 alterations as a prognostic factor. It is plausible that cell context-specific differences in pathways downstream of p53 may also play a role.

Direct targets of p53 include DNA sequences coding for microRNAs (miRNAs). miRNAs are single-stranded, noncoding RNAs of 18–24 nucleotides which have recently been shown to regulate protein expression. miRNAs bind to specific mRNAs, thereby blocking translation and increasing degradation.⁷ Several of these mRNA targets code for proteins with oncogene and tumor suppressor functions;^{8,9} therefore, by affecting the translation of these genes, miRNAs may play a key role in cellular transformation^{10,11} and tumor metastasis.¹²

Members of the miR-34 family (miR-34a, miR-34b and miR-34c) are direct miRNA targets of p53 and represent potential tumor suppressors.^{13–18} Expression of these miRNAs appears to be epigenetically regulated. DNA methylation of miR-34b/c has been found in colorectal cancer as well as in melanoma, in which methylation of CpG islands correlates with decreased expression and increased metastatic potential.^{19,20} This effect may be mediated by the MET proto-oncogene, which has been identified as a putative target gene of miR-34a.¹⁴

MET encodes the hepatocyte growth factor receptor, a tyrosine kinase that is associated with invasive ability, cell growth, angiogenesis and scattering.²¹ Numerous studies have shown that invasive growth is attenuated by the inhibition of MET expression, indicating a close relationship between MET and invasive properties.^{22,23} It is unclear, however, if MET plays a role in ESC.

To investigate whether a relationship existed between miRNA and tumor behavior, we obtained miRNA profiles of endometrial carcinomas using an miRNA microarray. We then sought to identify specific miRNAs, and target mRNAs associated with invasiveness and p53 mutation in ESC. Finally, we investigated how these miRNAs affected the function of endometrial cancer cells.

Material and Methods

Cell lines

Four human endometrial cancer cell lines (Ishikawa, RL95-2, SPAC-1-L and USPC-1) were examined in this study. Ishikawa cells were provided by Dr. Nishida from the Department of Obstetrics and Gynecology, Institute of Clinical Medicine, University of Tsukuba (Ibaraki, Japan). RL95-2 cells were obtained from the American Type Culture Collection (Rockville, MD). Established human endometrial serous carcinoma cell lines were provided by the laboratory of Dr. Hirai (SPAC-1-L), Department of Gynecology, Cancer Institute Hospital (Tokyo, Japan)²⁴ and Dr. Santin (USPC-1), Department of Obstetrics and Gynecology, Division of Gynecologic Oncology at the Yale University School of Medicine (New Haven, CT).²⁵ All cell lines were cultured in the appropriate medium and passed at confluence on 10 cm² dishes (Becton Dickinson and Co., Lincoln Park, NJ). The dishes were cultured in a 37°C incubator supplied with humidified 5% CO₂ and 95% air. The medium was changed twice a week.

Cells were incubated in growth medium with or without the DNA demethylating agent, 1 μM 5-aza-2'-deoxycytidine (DAC; Sigma-Aldrich, St. Louis, MO), for 72 hr, replacing the drug and medium every 24 hr. For histone deacetylase inhibition, 0.5 μM trichostatin A (TSA; Sigma-Aldrich) was added for the final 16 hr.

Tissue samples

After obtaining informed consent, 21 serous adenocarcinoma tissues, 20 endometrioid adenocarcinoma tissues, and 7 normal endometrial tissues (four proliferative phases and three secretory phases) were retrieved from the surgical pathology files at Tohoku University Hospital (Sendai, Japan). The research protocol was approved by the Ethics Committee at Tohoku University Graduate School of Medicine (Sendai, Japan). All surgical specimens were collected between January 2001 and December 2006 at Tohoku University Hospital (Sendai, Japan). Only patients diagnosed with a pure adenocarcinoma without other histological elements were included. The clinical data and patient characteristics are shown in Supporting Information, Table S1. We also obtained control normal endometrial tissue samples from hysterectomy specimens obtained from patients who underwent surgery for benign conditions. No patients had received preoperative radiotherapy or chemotherapy. The lesions were classified using World Health Organization criteria and were staged according to the International Federation of Gynecology and

Obstetrics system.^{26,27} The specimens were processed in 10% formalin, fixed for 24–48 hr, paraffin embedded, and thin-sectioned (3 μm). Frozen archival specimens were embedded immediately upon collection in optimal cutting temperature (OCT) compound (Sakura Finetechnical, Tokyo, Japan) and stored at –80°C for further use. Only sections containing a minimum of 90% carcinoma by examination with hematoxylin–eosin staining were used for total RNA and DNA preparation. Total RNA, including miRNA, was extracted using QIAzol Lysis reagent (Qiagen, Valencia, CA) and the miR-Neasy Mini Kit (Qiagen) according to the manufacturer's instructions. Genomic DNA was extracted using a QIAamp DNA Mini Kit (Qiagen).

Immunohistochemistry

Immunohistochemical analysis was performed with the streptavidin–biotin amplification method using a Histofine kit (Nichirei, Tokyo, Japan). A monoclonal antibody for p53 (B20.1) and a polyclonal antibody for MET (SP260) were purchased from Biomedica (Foster City, CA) and Santa Cruz Biotechnology, respectively. For immunostaining, the slides were heated in an autoclave at 121°C for 15 min for p53, and in a microwave for 20 min for MET in 0.01 M citric acid buffer following deparaffinization for antigen retrieval. The dilutions of primary antibodies for p53 and MET were 1:50 and 1:100, respectively. The antigen–antibody complex was visualized with 3,3'-diaminobenzidine solution and counterstained with hematoxylin. Tissue sections of colon cancer and breast cancer were used as positive controls for p53 and MET, respectively. For p53 expression, tumor cells were considered positive when more than 10% of the tumor cells showed nuclear staining. For MET expression, the distribution and intensity were scored according to methods which have been described previously.²⁸ The percentage of positive cells was classified as 0 (none), 1 (<1%), 2 (2–10%), 3 (11–33%), 4 (34–66%) and 5 (>67%). The immunointensity was classified as 0 (negative), 1 (very weak), 2 (weak), 3 (moderate), 4 (strong) and 5 (very strong). The total score of cell was obtained by adding the immunostaining score and the immunointensity score (range, 0–10). Scores from 2 to 10 were regarded as positive, whereas scores from 0 to 1 were regarded as negative. The immunohistochemical expression was independently reviewed by two of the authors (E. H. and J. A.).

miRNA microarray analysis

RNA purity and concentration were confirmed using the Agilent 2100 Bioanalyzer (Agilent Technologies, Santa Clara, CA). miRNA microarrays were manufactured by Agilent Technologies and contained 20–40 features targeting each of 470 human miRNAs. Labeling and hybridization of total RNA samples (100 ng) were performed according to the manufacturer's protocol. The arrays were scanned with an Agilent microarray scanner (Agilent Technologies) using high dynamic range settings as specified by the manufacturer.

Microarray results were extracted using Agilent Feature Extraction software Ver. 9.5.3.1 (Agilent Technologies) and analyzed using Gene Spring GX 7.3.1 software (Agilent Technologies) to obtain gene expression ratios. Microarray data have been submitted to the GEO database (GSE25405).

Quantitative real-time reverse transcription polymerase chain reaction

Quantitative reverse transcription polymerase chain reaction (RT-PCR) analysis was performed using Taqman MicroRNA Assays (Applied Biosystems, Foster City, CA), according to the manufacturer's protocol. Five nanograms of total RNA was used for the synthesis of first-strand cDNA using the TaqMan MicroRNA Reverse Transcription Kit (Applied Biosystems) following the manufacturer's instructions. Real-time PCR analyses were performed on an ABI7500 thermalcycler (Applied Biosystems), using TaqMan probes hsa-mir-34b and RNU6B. The fold-change for miRNA, relative to RNU6B, was calculated using the $2^{-\Delta\Delta C_t}$ method.²⁹ Three independent RT-PCR reactions were performed.

Western blot analysis

Cell protein was extracted using M-PER Mammalian Protein Extraction Reagent (Pierce Biotechnology, Rockford, IL) with Halt Protease Inhibitor Cocktail (Pierce Biotechnology). Ten micrograms of protein (whole cell extracts) was subjected to Poly-Acrylamide Gel Electrophoresis (SDS-PAGE) (10% acrylamide gel). Following SDS-PAGE, proteins were transferred onto Hybond P polyvinylidene difluoride membrane (GE Healthcare, Buckinghamshire, UK). The membrane was then washed with tris buffered saline (TBS) containing 0.1% Tween 20 (TBS-T) and blocked in TBS-T containing 5% skim milk. The membrane was probed with primary antibodies for MET (Cell Signaling Tech, Danvers, MA) and β -actin (Sigma-Aldrich) for 1 hr at room temperature. Primary antibodies were diluted as follows: MET 1/1,000 and β -actin 1/10,000. After incubation with antimouse IgG horseradish peroxidase (GE Healthcare) for 1 hr at room temperature, antibody-protein complexes on the blots were detected using ECL-plus Western blotting detection reagents (GE Healthcare). The protein bands were visualized with the LAS-1000 image analyzer (Fuji Photo Film, Tokyo, Japan).

Methylation analysis

One microgram of genomic DNA was treated with sodium bisulfite using the EpiTect Bisulfite Kit (Qiagen) according to the manufacturer's instructions. Bisulfite colony sequence analysis was carried out in endometrial cancer cell lines and bisulfite direct sequence analysis in normal and tumor specimens. The primer sequences were designed using Meth Primer (<http://www.urogene.org/methprimer/>). Hot-start PCR was performed at 95°C for 2 min, followed by 40 cycles of denaturation at 95°C for 30 sec, annealing at 55°C for 30 sec and elongation at 72°C for 1 min. The correctly sized band was isolated and its DNA was extracted using the QIAquick

Gel Extraction Kit (Qiagen). Amplified bisulfite-sequencing PCR products were cloned into the T-easy vector (Promega, Madison), and 10 clones from each sample were sequenced using an ABI3100 Genetic Analyzer (Applied Biosystems) according to the manufacturer's instructions.

PCR and p53 gene mutation analysis

TP53 exons 5–8 were amplified using primers which are described elsewhere.³⁰ Amplification reactions (20 μ L) contained 10 ng of DNA and 3.2 pmol of each primer according to the manufacturer's instructions. The amplifications were performed with a DNA Engine Tetrad, PTC-225 thermal cycler (Biorad, Hercules, CA). PCR products were purified using the NucleoFast 96 PCR plates from Macherey-Nagel using the manufacturer's protocol. Purified PCR products were sequenced using the ABI Prism BigDye terminator v3.1 chemistry (Applied Biosystems) and an ABI 3100 genetic analyzer (Applied Biosystems). The results were analyzed using Seq-Scape v1.0 (Applied Biosystems). Sequencing reactions were performed in both the forward and reverse directions. All sequences were manually examined. All exons with a mutation were reamplified and resequenced in two directions.

Transfection of precursor miRNA

SPAC-1-L cells (1×10^5) and USPC-1 cells (1×10^5) were transfected with 100 pmol of Pre-miR miRNA Precursor Molecules (Applied Biosystems) or Pre-miR miRNA Molecules Negative Control 1 or 2 (Applied Biosystems) using LipofectamineRNAiMAX (Invitrogen, Carlsbad, CA) according to the manufacturer's instructions. For the Western blot analysis and biological assays, cells were used 72 hr after transfection.

Cell proliferation assay, apoptosis assays, migration assay and invasion assay

Cell number was evaluated indirectly using a Cell Counting Kit-8 (Dojindo, Kumamoto, Japan) according to the manufacturer's instructions. The apoptotic status of cells was evaluated using a Caspase-3/7 Glo Assay (Promega) according to the manufacturer's instructions. Fluorescence was obtained with a Model 680 microplate reader (Bio-Rad Laboratories, Hercules, CA). Detection of apoptosis by flow cytometry was performed using the Annexin V-FITC Apoptosis Detection Kit (MBL, Nagoya, Japan). The staining was performed according to the manufacturer's instructions. Ten thousand cells per sample were analyzed using a BD FACSCantoTMII flow cytometer (BD Biosciences). For transwell migration assays, 5×10^4 cells were plated in the top chamber with a noncoated membrane (24-well insert; pore size, 8 μ m; BD Biosciences, Two Oak Park, MA). For invasion assays, 5×10^4 cells were plated in the top chamber with a Matrigel-coated membrane (24-well insert; pore size, 8 μ m; BD Biosciences). In both assays, cells were plated in serum-free medium containing 1% bovine serum albumin (BSA), and medium supplemented with serum was used as a

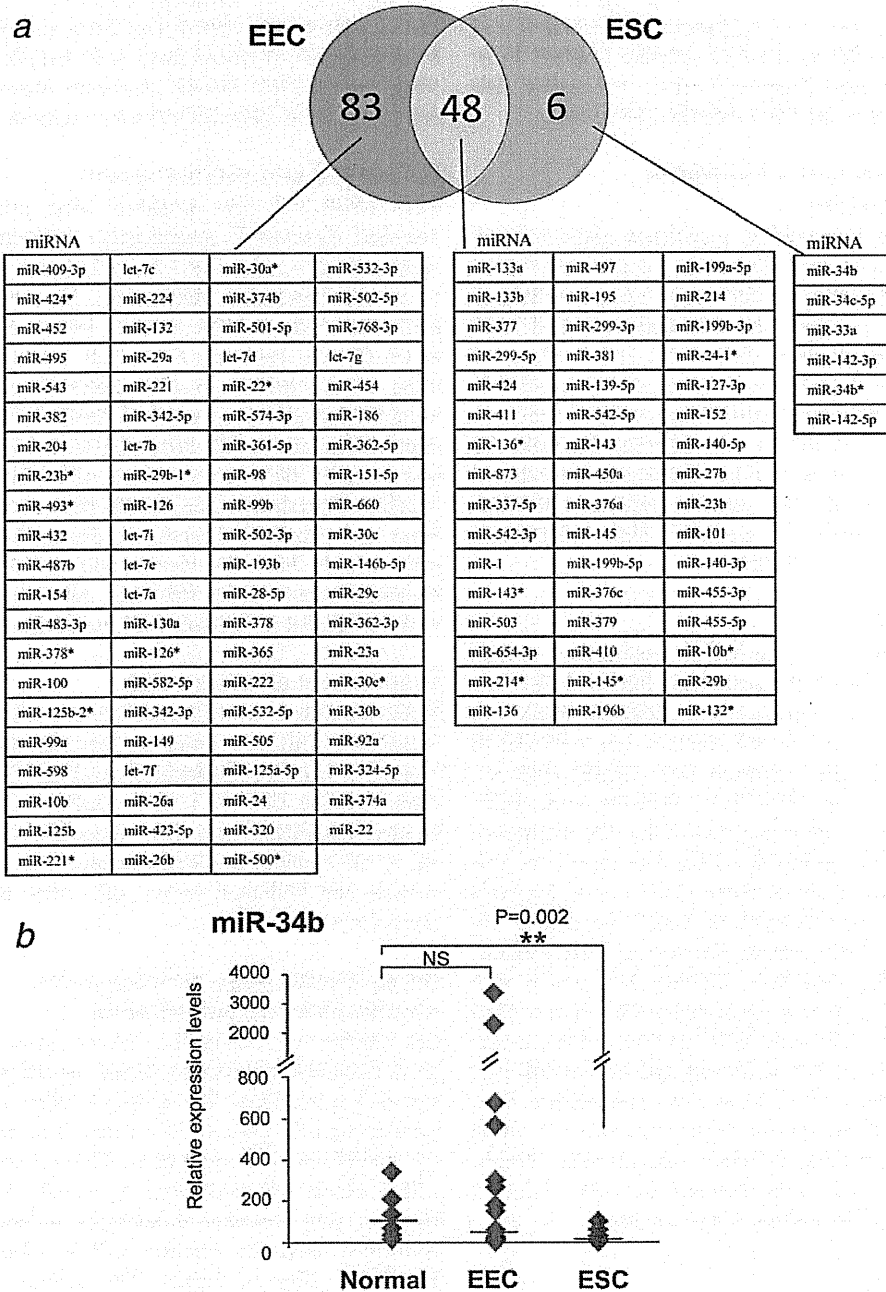


Figure 1. (a) miRNAs that exhibited a statistically significant decrease relative to normal endometria. Six genes (pink) were specifically down-regulated in ESC. (b) Quantitative real-time RT-PCR of miR-34b microarray data. Expression of miR-34b was significantly down-regulated in ESC. Columns, means of three replicates. Normal, normal endometrial tissues. $**p < 0.01$; NS, nonsignificant. [Color figure can be viewed in the online issue, which is available at wileyonlinelibrary.com.]

chemoattractant in the lower chamber. The cells were incubated for 6 hr at 37°C for the migration assay and 24 hr at 37°C for the invasion assay. Cells which did not migrate or invade through the pores were removed by a cotton swab, and those on the lower surface were subsequently fixed with

methanol and stained with toluidine blue O. The migration or invasive ability was evaluated as the total number of cells on the lower surface of the membrane as determined by microscopy. All functional analyses were performed in duplicate and repeated independently three times.

Statistical analysis

Raw microarray data were normalized and analyzed using Gene Spring GX 7.3.1 software (Agilent Technologies). Expression data were median centered. Statistical analysis was performed using SAS software version 5.0 (Statview, Cary, NC). miRNAs that had a greater than twofold change were considered to have significant differential expression compared to normal endometria. The Mann–Whitney *U* test was performed to identify miRNAs that demonstrated statistically significant differential expression, and to evaluate differences between miRNA expression and immunohistochemical expression. Results were expressed as means \pm SD and analyzed by one-way analysis of variance (ANOVA) and the Bonferroni test for functional analyses. $p < 0.05$ was considered to be statistically significant.

Results

Analysis and comparison of miR-34b expression in ESC tissues, EEC tissues and normal endometrial tissues

miRNA microarray analysis was used to identify miRNAs that were differentially expressed among ESC, EEC, and normal endometria. We focused on down-regulated miRNAs as many are regulated by P53. Figure 1a shows the miRNAs exhibiting statistically significant down-regulation in ESC and EEC compared to normal endometrial tissues. A total of 54 miRNAs were down-regulated in ESC, and 131 in EEC. Forty-eight miRNAs were commonly down-regulated in ESC and EEC. Notably, six miRNAs were specifically down-regulated in ESC. Of these six miRNAs, miR-34b displayed the greatest degree of down-regulation (40.2-fold; Table 1). Down-regulation of miR-34b was validated by quantitative RT-PCR which confirmed significant down-regulation in ESC (35.8-fold, $p = 0.002$), and no significant down-regulation in EEC (2.9-fold, NS; Fig. 1b).

We next investigated whether a correlation existed between miR-34b expression in ESC and clinicopathological features (clinical stage, myometrial invasion, lymph node metastasis and degrees of vascular invasion) and found no statistically significant associations (data not shown). p53 immunoreactivity was detected in the nuclei of 18 out of 21 (85.7%) ESC cases (Supporting Information, Table S1 and Fig. S1), while all normal endometrial tissues were negative. Lower expression of miR-34b tended to be inversely correlated with p53 immunohistochemical overexpression; however, this finding was not statistically significant (data not shown).

Analysis of miR-34b CpG island DNA methylation in endometrial cancer cell lines and primary ESC

To determine whether miR-34b down-regulation was explained by DNA methylation, we performed bisulfite sequencing of endometrial cancer cell line genomic DNA. This analysis revealed that the CpG sites in this region were extensively methylated in RL95-2 and SPAC-1-L cells, whereas moderate methylation was seen in USPC-1 cells. In

Table 1. Specially down-regulation expression miRNAs in ESC versus normal endometrial tissue

miRNA	Fold change	<i>p</i> value
miR-34b	40.2	0.014
miR-34c-5p	6.17	0.014
miR-33a	6.1	0.002
miR-142-3p	3.18	0.005
miR-34b*	2.97	0.016
miR-142-5p	2.69	0.01

Significant *p* value ($p < 0.05$).

contrast, only a low level of methylation was seen in Ishikawa cells (Fig. 2a). The average methylation levels in Ishikawa, RL95-2, SPAC-1-L and USPC-1 cells were 10, 96, 76 and 25%, respectively (Table 2).

We next analyzed the miR-34b methylation pattern in tumor specimens from ESC patients. Bisulfite sequencing revealed that miR-34b was methylated in 37% of the ESC specimens and in 60% of EEC. In contrast, only a low level of methylation (6%) was detected in normal endometrial samples, indicating that methylation of the miR-34b region is a tumor-specific phenomenon (Fig. 2a).

We next analyzed four endometrial cancer cell lines (Ishikawa, RL95-2, SPAC-1-L and USPC-1), which were treated with or without DAC and TSA. We found that miR-34b was markedly up-regulated or re-expressed by DAC in RL95-2, SPAC-1-L and USPC-1. Up-regulation did not occur in Ishikawa cells. DAC treatment produced increases in miR-34b expression of the following magnitudes: RL95-2, 9.3-fold; SPAC-1-L, re-expression and USPC-1, 36.5-fold (Fig. 2b). The outcomes were similar for DAC alone and combined TSA and DAC treatment in all cell-lines; however, TSA alone failed to produce either up-regulation or re-expression (Fig. 2b). Correlations of the status of miR-34b promoter methylation with p53 mutation, and miR-34b expression level in these cell lines are shown in Table 2.

Restoration of miR-34b inhibited growth, migration and invasion and promoted apoptosis activity of ESC cells

To determine whether miR-34b suppressed cancer cell growth, SPAC-1-L and USPC-1 cells were transfected with miR-34b precursor molecules or a negative control. Statistically significant reductions in proliferation by 8.3% ($p = 0.003$) and 16.1% ($p = 0.002$) in comparison to the control were observed on miR-34b transfection of SPAC-1-L and USPC-1 cells, respectively (Fig. 3a). As this may have been the result of apoptosis, we measured caspase activity. As shown in Figure 3b, overexpression of miR-34b precursor molecules led to a statistically significant increase in caspase 3/7 activity (NC 247.8 ± 6.8 vs. miR-34b 284.4 ± 17.7 , $p = 0.03$ in SPAC-1-L and NC 4783.0 ± 339.4 vs. miR-34b 9589.7 ± 748.5 , $p = 0.001$ in USPC-1). miR-34b precursor molecules also produced caspase 3/7 increases in SPAC-1-L

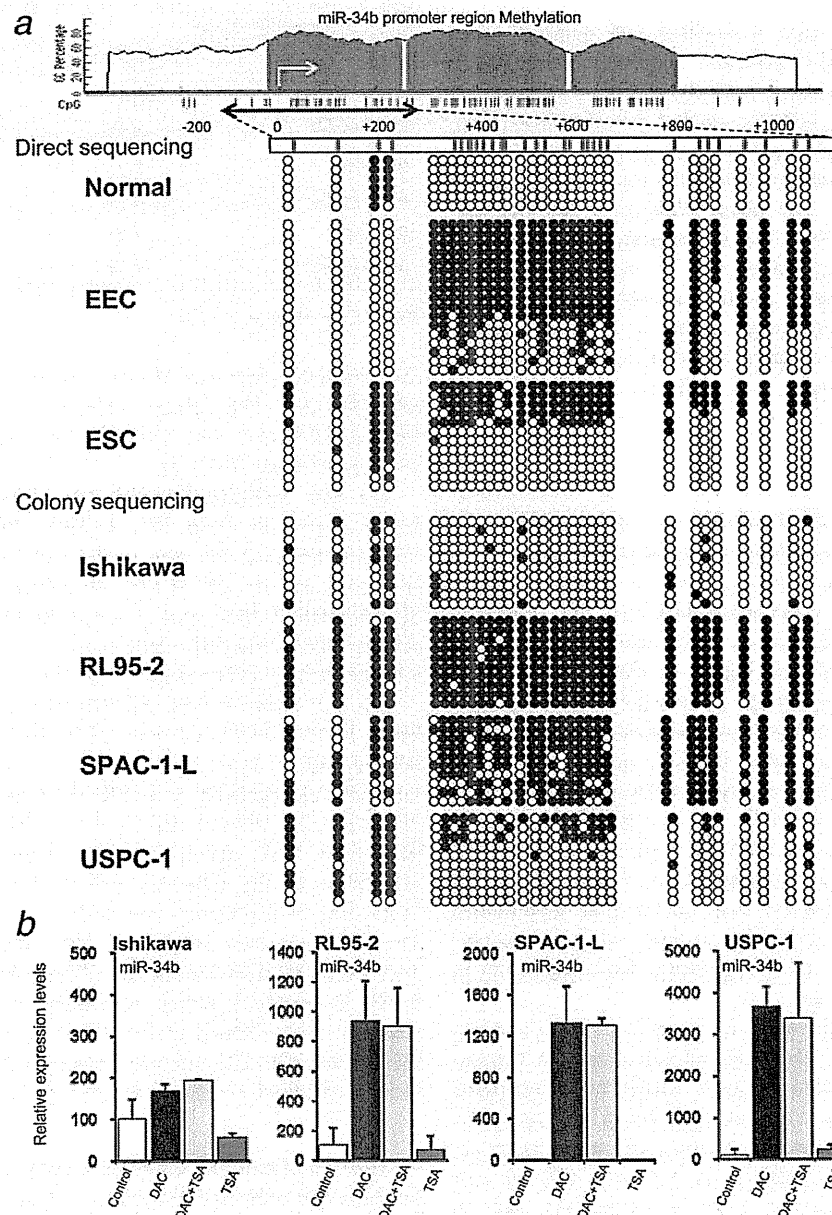


Figure 2. (a) Methylation status of the miR-34b promoter region determined by bisulfite sequencing in primary endometrial adenocarcinoma specimens and normal endometrial tissues, and bisulfite sequencing of clonal populations of endometrial cancer cell lines. In cell lines, 10 single clones are represented for each sample. Methylation status of 31 CpG sites detected by bisulfite sequencing is displayed. Solid circles (●) indicate the methylated CpG sites; open circles (○), unmethylated sites. Normal, normal endometrial tissues. (b) Quantitative RT-PCR results for miR-34b in the indicated endometrial cancer cell lines, with and without DAC and/or TSA treatment. Results are normalized to internal U6 snRNA expression. Columns, means of three replicates; error bars, standard deviations. [Color figure can be viewed in the online issue, which is available at wileyonlinelibrary.com.]

and USPC-1 cells in comparison to the precursor-transfected negative control, as assessed by flow cytometry.

In a migration assay, a 42% decrease in SPAC-1-L ($p = 0.001$) and 16.6% decrease in USPC-1 ($p = 0.006$) were observed on transfection of the miR-34b precursor (Fig. 3d).

In the invasion assay, an 80% decrease in SPAC-1-L ($p < 0.0001$) and 78.7% decrease in USPC-1 ($p = 0.0004$) were observed (Fig. 3e). The most striking decrease was observed in invasion assays after miR-34b precursor molecules were transfected into SPAC-1-L cells.

Table 2. The status of methylation of miR-34b promoter, p53 mutation and miR-34b expression level in the cell lines

Cell line	Methylation of miR-34b promoter (%)	miR-34b relative expression level	Status of p53 mutation	Exon	Protein change
Ishikawa	10	525.7	(+) p	7	M246X
RL95-2	96	3.3	(+) d	6	V218-
SPAC-1-L	76	1	(+) p	8	P273X
USPC-1	25	10.1	(+) p	7	R248W

p, point mutation; d, deletion.

Correlation between miR-34b expression and MET protein expression in endometrial cancer cell lines and primary ESC

To evaluate if miR-34b modulated the level of MET in SPAC-1-L and USPC-1 cells, MET expression was measured by Western blotting after transfection with miR-34b precursor molecules. As shown in Figure 4a, 72 hr after miR-34b transfection, the amount of MET protein was significantly reduced in both cell lines.

MET immunoreactivity was detected in both the membrane and the cytoplasm of cancer cells (Fig. 4b). Greater reactivity was noted in the infiltrating cells at the tumor periphery. Patients with ESC were subdivided into three subgroups: negative/lower positive; negative and strongly positive and positive.²⁸ Fourteen out of 21 (66.7%) ESC cases were positive for MET immunoreactivity (Supporting Information, Table S1). In contrast, all normal cases were negative. Lower expression of miR-34b was significantly correlated with MET overexpression ($p = 0.012$; Fig. 4c).

Discussion

Our study demonstrated that miR-34b expression was significantly down-regulated in ESC tissues compared with normal endometrial tissues. In addition, there was a significant correlation between negatively regulated miR-34b expression and the rate of positive MET immunostaining. Negatively regulated miR-34b was associated with CpG island hypermethylation, as demethylation by DAC restored the expression of miR-34b. Restoration of miR-34b induced apoptosis and inhibited cell growth, migration and most notably invasion. In addition, MET protein expression was reduced by the restoration of miR-34b expression. To our knowledge, our report is the first one examining the effect of ectopic miR-34b expression on cancer cell behavior in ESC.

ESC is characterized by a high rate of p53 mutation.⁴ p53 directly inhibits the expression of miR-34b/c and miR-34a in addition to its classical effect of inducing p21 expression and arresting the cell cycle.¹³⁻¹⁸ miR-34a is encoded by a unique transcript, whereas mi-34b and miR-34c share a common primary transcript.³¹ In ESC cases, our miRNA microarray analysis revealed that miR-34b was the second most down-regulated gene (40.2-fold compared with the normal endometrial tissue) and that miR-34c-5p was the 33rd most down-

regulated gene (6.2-fold). The reverse strand of miR-34b* was also decreased 3.0-fold.³² The other three miRNAs exhibited concomitant down-regulation, suggesting that they were polycistronic. In addition, miR-34b showed the greatest degree of specific down-regulation in ESC tissues compared with normal endometria. The alterations in gene expression were paralleled by the immunohistochemical data. miR-34b expression was low in ESC, in which immunostaining was strongly positive for p53, and higher in tumor samples without abnormal p53 accumulation. It is plausible that the down-regulation of miR-34b expression results from p53 dysfunction, as miR-34b is the target of p53.¹³⁻¹⁸

Dysregulation of miRNA expression occurs through several mechanisms including the gain or loss of gene copy number,³³ structural mutations (germline mutations) in miRNA precursor molecules,³⁴ promoter methylation,³⁵ abnormal miRNA processing³⁶ and transcriptional regulators.¹³ Besides p53 mutation, epigenetic regulation has recently been identified in miR-34b. Specifically, hypermethylation of the miR-34b/c promoter region has been found in a number of tumor types.^{19,37} In melanoma, a correlation has been shown between methylation status and metastatic potential.²⁰ In nonsmall cell lung cancer, however, Boomer *et al.* demonstrated that loss of miR-34b expression was correlated with p53 deletion and not with CpG methylation.¹⁵ Thus, multiple mechanisms are thought to exist for the regulation of miR-34b expression. In our study, miR-34b promoter hypermethylation was observed in both EEC and ESC and at a lower frequency in ESC. In both EEC- and ESC-derived cell lines, the use of a demethylating agent restored miR-34b expression which had been low due to hypermethylation indicating that methylation was likely responsible for down-regulation of miR-34b in both lines. Further studies are needed to ascertain whether both p53 mutation and promoter methylation are contributing to the aberrant miR-34b expression found in ESC.

miR-34b/c modulates cell proliferation and regulates the cell cycle in a manner consistent with a tumor suppressor. Ectopic miR-34b/c expression in IM90 fibroblast cells decreases growth and induces senescence.¹⁴ Additionally, in a variety of cancer cells, ectopic miR-34b/c expression induces G1 cell-cycle arrest.^{14,15,18} Anchorage independent growth is also inhibited by miR-34b/c.¹³ Our results were consistent in that restoration of miR-34b slightly but significantly reduced cell growth, suggesting an indirect effect.

In our study, apoptosis may have contributed to the decrease in cell number following ectopic expression of miR-34b/c. This is similar to what has been observed in nonsmall lung cancer cells in which miR-34a presumably interacts with other apoptotic pathway genes.¹⁶ Similarly, our results indicated that miR-34b cooperated with other factors to promote apoptosis in ESC. However, the increase of apoptosis was moderate, which suggested that this phenotype was an indirect effect.

A clinically significant finding was that miR-34b in the ESC cells significantly inhibited migration and invasion. Our results showed that the inhibitory effects of miR-34b were more

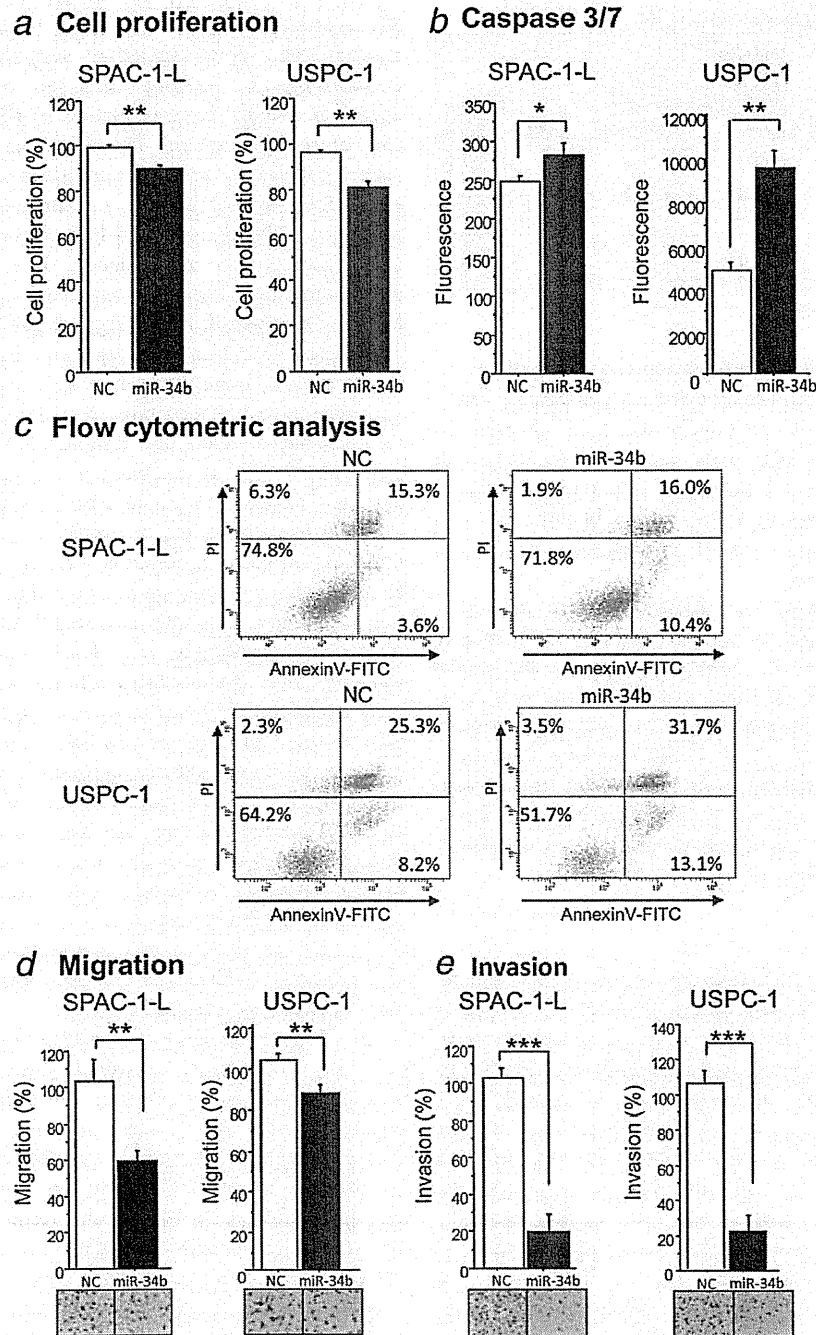


Figure 3. SPAC-1-L cells and USPC-1 cells were transfected with pre-miR-34b precursor molecules, or a negative control for 72 hr. (a) Cell proliferation assay; (b) Caspase 3/7 Glo assay. NC, transfected with negative control; 34b, transfected with pre-miR-34b molecules. Columns, means of three replications; error bars, standard deviations. * $p < 0.05$, ** $p < 0.01$ and *** $p < 0.001$ versus controls. (c) Flow cytometric analysis. Cell death was monitored by Annexin V staining and flow cytometry. The right lower quadrant of each plot contains early apoptotic cells, whereas the right upper quadrant contains late apoptotic cells. This experiment was repeated three independent times and similar results were obtained each time. PI, propidium iodide. (d) Migration assay; (e) invasion assay. NC, transfected with negative control; miR-34b, transfected with pre-miR-34b molecules. Columns, means of three replications; error bars, standard deviations. ** $p < 0.01$ and *** $p < 0.001$ versus controls. Fields shown in the figure are representative of three replications. [Color figure can be viewed in the online issue, which is available at wileyonlinelibrary.com.]

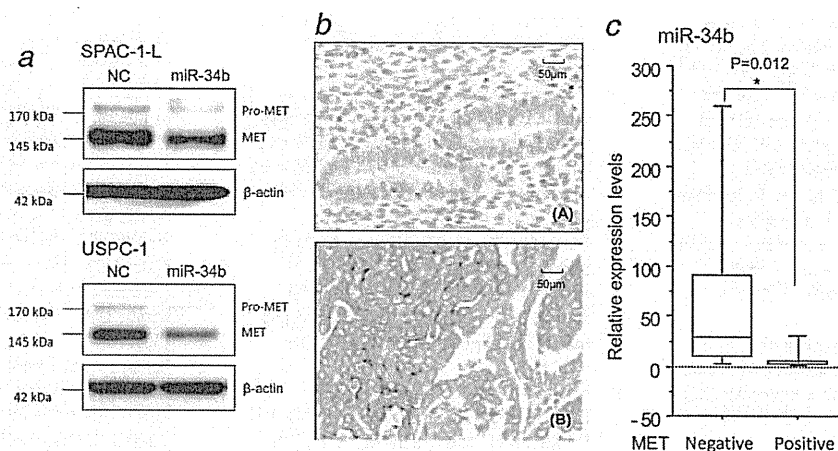


Figure 4. (a) Immunoblotting for MET in SPAC-1-L and USPC-1 cells. Specific bands corresponded to MET and β -actin immunoreactivity (approximately 145 and 42 kDa, respectively). MET antibody recognized both pro-MET and mature MET (approximately 175 and 145 kDa, respectively). MET immunoreactivity was clearly diminished in cells transfected with pre-miR-34b precursor molecules after 72 hr compared with negative control cells. NC, transfected with negative control; miR-34b, transfected with pre-miR-34b molecules. (b) Immunohistochemistry of MET expression in ESCs: (A) MET immunoreactivity was negative in all normal endometrial tissues and (B) MET immunoreactivity was detected in both the membrane and the cytoplasm of cancer cells. Original magnification, 200 \times for (A) and (B). (c) miR-34b expression was significantly lower in tissues exhibiting positive MET immunoreactivity. Negative, MET negative and weakly positive immunoreactivity; Positive, MET strongly positive immunoreactivity. Columns, means of three replicates; error bars, standard deviations. * $p < 0.05$.

pronounced in ESC than in EEC. It is plausible that these observations are the result of alterations in the expression of genes that are downstream targets of miR-34b.

MET, c-MYC, CDK6 and CREB are putative target genes of miR-34b.³⁸ Of these, MET, through activation, is involved in several critical steps in tumor development and metastatic dissemination.²² MET is a direct target of the miR-34 family in ovarian cancer cells.^{23,39} miR-34b/c binds to the 3'UTR of MET and impairs MET mRNA translation.^{19,23,39} Furthermore, the migratory and invasive activities of the cancer cells are controlled by the negative regulation of MET *via* miR-34b/c.^{23,39}

MET expression is a significant prognostic factor in EEC patients.⁴⁰ Consistent with these results, we obtained markedly reduced levels of MET protein by transfection of miR-34b precursor molecules. This suggests that MET is in part responsible for the invasive behavior of ESC cell lines. Additionally, MET overexpression correlated with miR-34b reduction in primary cancer specimens. These results suggest that miR-34b might function as a tumor suppressor by regulating invasive growth *via* MET. To our knowledge, this report is the first to show the correlation between miRNA-mediated MET expression and invasion in ESC cells.

Our findings, taken together with the previously discussed studies, suggest that miRNAs such as miR-34b/c have a tumor suppressive function. Therefore, this pathway may represent a

potential therapeutic target. Preliminary studies have already been completed in xenograft models. For example, the administration of a miR-34a/atelocollagen complex has been shown to inhibit tumor growth of colon cancer cell lines in xenograft models.⁴¹ The reintroduction of miR-34b/c has been reported to inhibit the migratory ability, tumor growth and metastasis formation in head and neck cancer lines in xenograft models.²⁰ Further studies are needed to determine whether restoration of miR-34 will have a therapeutic role in ESC.

In conclusion, we have shown that miR-34b is down-regulated in endometrial carcinomas. The inhibition of cell growth and increase in apoptosis were confirmed by transfection of the miR-34b. Although the effect was statistically significant, the overall magnitude was weak. Therefore, the actions of miR-34b are likely indirect. miR-34b down-regulation is also associated with increased migration and invasion, suggesting that this pathway is involved in the aggressive behavior of ESC. Further studies are needed to verify whether this pathway represents a viable therapeutic target.

Acknowledgements

The authors express their sincere appreciation to Dr. M. Nishida for the Ishikawa cell line, Dr. Y. Hirai for the SPAC-1-L cell line and Dr. A.D. Santin for the USPC-1 cell line. They thank Dr. T. Mutou and Dr. M. Matsumoto for their technical support.

References

1. Bancher-Todesca D, Neunteufel W, Williams KE, Prainsack D, Breitenacker G, Friedlander ML, Hacker NF. Influence of postoperative treatment on survival in patients with uterine papillary serous carcinoma. *Gynecol Oncol* 1998;71:344–7.
2. Lauchlan SC. Tubal (serous) carcinoma of the endometrium. *Arch Pathol Lab Med* 1981;105:615–8.

3. Hamilton CA, Cheung MK, Osann K, Chen L, Teng NN, Longacre TA, Powell MA, Hendrickson MR, Kapp DS, Chan JK. Uterine papillary serous and clear cell carcinomas predict for poorer survival compared to grade 3 endometrioid corpus cancers. *Br J Cancer* 2006;94:642–6.
4. Tashiro H, Isacson C, Levine R, Kurman RJ, Cho KR, Hedrick L. p53 gene mutations are common in uterine serous carcinoma and occur early in their pathogenesis. *Am J Pathol* 1997;150:177–85.
5. Lax SF. Molecular genetic pathways in various types of endometrial carcinoma: from a phenotypical to a molecular-based classification. *Virchows Arch* 2004;444:213–23.
6. Finlay CA, Hinds PW, Tan TH, Eliyahu D, Oren M, Levine AJ. Activating mutations for transformation by p53 produce a gene product that forms an hsc70-p53 complex with an altered half-life. *Mol Cell Biol* 1988;8:531–9.
7. Hannon GJ. RNA interference. *Nature* 2002;418:244–51.
8. Ota A, Tagawa H, Karnan S, Tsuzuki S, Karpas A, Kira S, Yoshida Y, Seto M. Identification and characterization of a novel gene, C13orf25, as a target for 13q31–q32 amplification in malignant lymphoma. *Cancer Res* 2004;64:3087–95.
9. He L, Thomson JM, Hemann MT, Hernando-Monge E, Mu D, Goodson S, Powers S, Cordon-Cardo C, Lowe SW, Hannon GJ, Hammond SM. A microRNA polycistron as a potential human oncogene. *Nature* 2005;435:828–33.
10. Calin GA, Dumitru CD, Shimizu M, Bichi R, Zupo S, Noch E, Aldler H, Rattan S, Keating M, Rai K, Rassenti L, Kipps T, et al. Frequent deletions and down-regulation of micro-RNA genes miR15 and miR16 at 13q14 in chronic lymphocytic leukemia. *Proc Natl Acad Sci USA* 2002;99:15524–9.
11. Cimmino A, Calin GA, Fabbri M, Iorio MV, Ferracin M, Shimizu M, Wojcik SE, Aqeilan RI, Zupo S, Dono M, Rassenti L, Alder H, et al. miR-15 and miR-16 induce apoptosis by targeting BCL2. *Proc Natl Acad Sci USA* 2005;102:13944–9.
12. Ma L, Weinberg RA. Micromanagers of malignancy: role of microRNAs in regulating metastasis. *Trends Genet* 2008;24:448–56.
13. Corney DC, Flesken-Nikitin A, Godwin AK, Wang W, Nikitin AY. MicroRNA-34b and MicroRNA-34c are targets of p53 and cooperate in control of cell proliferation and adhesion-independent growth. *Cancer Res* 2007;67:8433–8.
14. He L, He X, Lim LP, de Stanchina E, Xuan Z, Liang Y, Xue W, Zender L, Magnus J, Ridzon D, Jackson AL, Linsley PS, et al. A microRNA component of the p53 tumour suppressor network. *Nature* 2007;447:1130–4.
15. Bommer GT, Gerin I, Feng Y, Kaczorowski AJ, Kuick R, Love RE, Zhai Y, Giordano TJ, Qin ZS, Moore BB, MacDougald OA, Cho KR, et al. p53-mediated activation of miRNA34 candidate tumor-suppressor genes. *Curr Biol* 2007;17:1298–307.
16. Raver-Shapira N, Marciano E, Meiri E, Spector Y, Rosenfeld N, Moskovits N, Bentwich Z, Oren M. Transcriptional activation of miR-34a contributes to p53-mediated apoptosis. *Mol Cell* 2007;26:731–43.
17. Chang TC, Wentzel EA, Kent OA, Ramachandran K, Mullendore M, Lee KH, Feldmann G, Yamakuchi M, Ferlito M, Lowenstein CJ, Arking DE, Beer MA, et al. Transactivation of miR-34a by p53 broadly influences gene expression and promotes apoptosis. *Mol Cell* 2007;26:745–52.
18. Tarasov V, Jung P, Verdoodt B, Lodygin D, Epanchintsev A, Menssen A, Meister G, Hermeking H. Differential regulation of microRNAs by p53 revealed by massively parallel sequencing: miR-34a is a p53 target that induces apoptosis and G1-arrest. *Cell Cycle* 2007;6:1586–93.
19. Toyota M, Suzuki H, Sasaki Y, Maruyama R, Imai K, Shinomura Y, Tokino T. Epigenetic silencing of microRNA-34b/c and B-cell translocation gene 4 is associated with CpG island methylation in colorectal cancer. *Cancer Res* 2008;68:4123–32.
20. Lujambio A, Calin GA, Villanueva A, Ropero S, Sanchez-Cespedes M, Blanco D, Montuenga LM, Rossi S, Nicoloso MS, Faller WJ, Gallagher WM, Eccles SA, et al. A microRNA DNA methylation signature for human cancer metastasis. *Proc Natl Acad Sci USA* 2008;105:13556–61.
21. Giordano S, Zhen Z, Medico E, Gaudino G, Galimi F, Comoglio PM. Transfer of motogenic and invasive response to scatter factor/hepatocyte growth factor by transfection of human MET protooncogene. *Proc Natl Acad Sci USA* 1993;90:649–53.
22. Birchmeier C, Birchmeier W, Gherardi E, Vande Woude GF. Met, metastasis, motility and more. *Nat Rev Mol Cell Biol* 2003;4:915–25.
23. Migliore C, Petrelli A, Ghiso E, Corso S, Capparuccia L, Eramo A, Comoglio PM, Giordano S. MicroRNAs impair MET-mediated invasive growth. *Cancer Res* 2008;68:10128–36.
24. Hirai Y, Kawaguchi T, Hasumi K, Kitagawa T, Noda T. Establishment and characterization of human cell lines from a serous papillary adenocarcinoma of the endometrium. *Gynecol Oncol* 1994;54:184–95.
25. Santin AD, Bellone S, Gokden M, Palmieri M, Dunn D, Agha J, Roman JJ, Hutchins L, Pecorelli S, O'Brien T, Cannon MJ, Parham GP. Overexpression of HER-2/neu in uterine serous papillary cancer. *Clin Cancer Res* 2002;8:1271–9.
26. Tavassoli FA, Devillee P, eds. Pathology and genetics tumours of the breast and female genital organs. World health organization classification of tumours. Lyon: IARC Press, 2003.
27. Creasman WT. Announcement, FIGO stages: 1988 reversions. *Gynecol Oncol* 1989.
28. Belfiore A, Gangemi P, Costantino A, Russo G, Santonocito GM, Ippolito O, Di Renzo MF, Comoglio P, Fiumara A, Vigneri R. Negative/low expression of the Met/hepatocyte growth factor receptor identifies papillary thyroid carcinomas with high risk of distant metastases. *J Clin Endocrinol Metab* 1997;82:2322–8.
29. Livak KJ, Schmittgen TD. Analysis of relative gene expression data using real-time quantitative PCR and the 2⁻(Delta Delta C(T)) method. *Methods* 2001;25:402–8.
30. Krypuy M, Ahmed AA, Etemadmoghadam D, Hyland SJ, DeFazio A, Fox SB, Brenton JD, Bowtell DD, Dobrovic A. High resolution melting for mutation scanning of TP53 exons 5–8. *BMC Cancer* 2007;7:168–80.
31. Hermeking H. The miR-34 family in cancer and apoptosis. *Cell Death Differ* 2010;17:193–9.
32. Hiroki E, Akahira J, Suzuki F, Nagase S, Ito K, Suzuki T, Sasano H, Yaegashi N. Changes in microRNA expression levels correlate with clinicopathological features and prognoses in endometrial serous adenocarcinomas. *Cancer Sci* 2010;101:241–9.
33. Zhang L, Huang J, Yang N, Greshock J, Megraw MS, Giannakakis A, Liang S, Naylor TL, Barchetti A, Ward MR, Yao G, Medina A, et al. microRNAs exhibit high frequency genomic alterations in human cancer. *Proc Natl Acad Sci USA* 2006;103:9136–41.
34. Calin GA, Ferracin M, Cimmino A, Di Leva G, Shimizu M, Wojcik SE, Iorio MV, Visone R, Sever NI, Fabbri M, Iuliano R, Palumbo T, et al. A MicroRNA signature associated with prognosis and progression in chronic lymphocytic leukemia. *N Engl J Med* 2005;353:1793–801.
35. Saito Y, Liang G, Egger G, Friedman JM, Chuang JC, Coetzee GA, Jones PA. Specific activation of microRNA-127 with downregulation of the proto-oncogene BCL6 by chromatin-modifying drugs in human cancer cells. *Cancer Cell* 2006;9:435–43.

36. Thomson JM, Newman M, Parker JS, Morin-Kensicki EM, Wright T, Hammond SM. Extensive post-transcriptional regulation of microRNAs and its implications for cancer. *Genes Dev* 2006;20:2202–7.
37. Vogt M, Munding J, Gruner M, Liffers ST, Verdoodt B, Hauk J, Steinstraesser L, Tannapfel A, Hermeking H. Frequent concomitant inactivation of miR-34a and miR-34b/c by CpG methylation in colorectal, pancreatic, mammary, ovarian, urothelial, and renal cell carcinomas and soft tissue sarcomas. *Virchows Arch* 2011; 458:313–22.
38. Griffiths-Jones S, Grocock RJ, van Dongen S, Bateman A, Enright AJ. miRBase: microRNA sequences, targets and gene nomenclature. *Nucleic Acids Res* 2006;34: D140–4.
39. Corney DC, Hwang CI, Matoso A, Vogt M, Flesken-Nikitin A, Godwin AK, Kamat AA, Sood AK, Ellenson LH, Hermeking H, Nikitin AY. Frequent downregulation of miR-34 family in human ovarian cancers. *Clin Cancer Res* 2010;16:1119–28.
40. Wagatsuma S, Konno R, Sato S, Yajima A. Tumor angiogenesis, hepatocyte growth factor, and c-Met expression in endometrial carcinoma. *Cancer* 1998;82: 520–30.
41. Tazawa H, Tsuchiya N, Izumiya M, Nakagama H. Tumor-suppressive miR-34a induces senescence-like growth arrest through modulation of the E2F pathway in human colon cancer cells. *Proc Natl Acad Sci USA* 2007;104: 15472–7.